Narodowe Laboratorium Technologii Kwantowych

dr hab. Jerzy Zachorowski

Opracowanie utworu pod tytułem:

"Podstawy technik doświadczalnych chłodzenia atomów" w ramach kursu zaawansowanego, organizowanego w dniach 31.08 – 25.09.09 będącego kontynuacją szkoleń z zakresu eksploatacji i zarządzania dużą infrastrukturą badawczą organizowanego przez Narodowe Laboratorium Technologii Kwantowych

INNOWACYJNA GOSPODARKA
NARODOWA STRATEGIA SPÓJNOŚCI

UNIA EUROPEJSKA
EUROPEJSKI FUNDUSZ ROZWOJU REGIONALNEGO

Projekt współfinansowany ze środków Europejskiego Funduszu Rozwoju Regionalnego w ramach Programu Operacjnego Innowacyjna Gospodarka

Narodowe
Laboratorium
Technologii
Kwantowych

INNOWACYJNA GOSPODARKA
NARODOWA STRATEGIA SPÓJNOŚCI

UNIA EUROPEJSKA
EUROPEJSKI FUNDUSZ
ROZWOJU REGIONALNEGO

Projekt współfinansowany ze środków Europejskiego Funduszu Rozwoju Regionalnego w ramach Programu Operacyjnego Innowacyjna Gospodarka

Experimental techniques of cooling and trapping

basic techniques and methods

Jerzy Zachorowski

Instytut Fizyki
Uniwersytet Jagielloński

INNOWACYJNA GOSPODARKA
NARODOWA STRATEGIA SPÓJNOŚCI

UNIA EUROPEJSKA
EUROPEJSKI FUNDUSZ
ROZWOJU REGIONALNEGO

Plan

- Lasers
- Atom sources
- Vacuum systems
- Magnetic fields
- Atom transfer
- Experiment control

Plan

- Lasers
  - requirements
  - basic types
  - stabilization
  - beam shaping
  - modulators

Lasers: requirements

- small spectral width, $\gamma_L < \Gamma$
- good frequency stability
- adequate power, ~100mW do 1W
- good power stability

Lasers: main types

- Diode lasers:
  Rb 780nm
  Cs 852nm
- Diode laser + (tapered) amplifier = MOPA
- Laser Ti: sapphire
- Dye laser

Diode laser

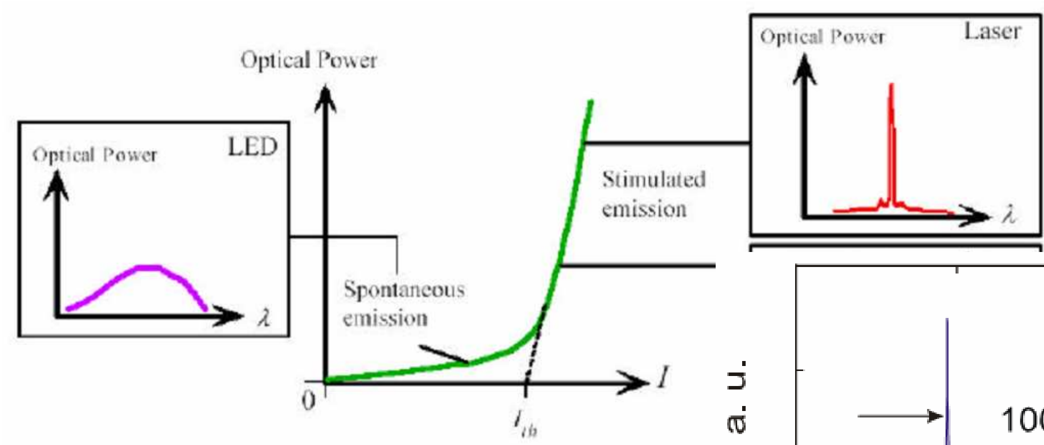

Lasing threshold and spectra

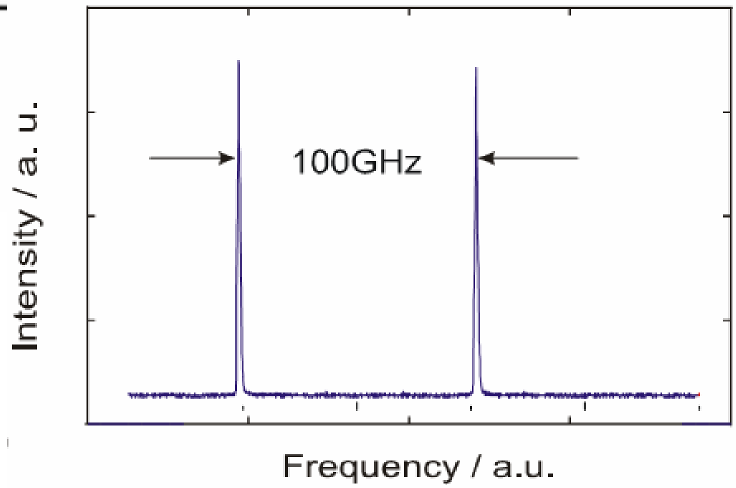

Well above threshold

Diode lasers: tuning

Temperature tuning: two effects on the emission of the laser diode:

1) Change of the refractive index of the laser material → shift of the lasing modes with the laser temperature.
   Temperature increase → increase of the wavelength .

2) Shift of the gain of the laser material → change of the emission wavelength of the laser diode.
   Temperature increase → increase of the wavelength of the laser gain.

Different slopes → mode hops

Example: Diode laser diodowy AlGaAs, 780 nm,

tuning slope: $d\lambda/dT = 0.06$ nm/K (continuous),

$d\lambda/dT = 0.25$ nm/K (overall)

Diode lasers: tuning

Current tuning: faster, smaller range, also changes power

tuning slope: dν/dI=3 GHz/mA (0.006 nm/mA)

Worst case scenario: mode hop at the desired wavelength

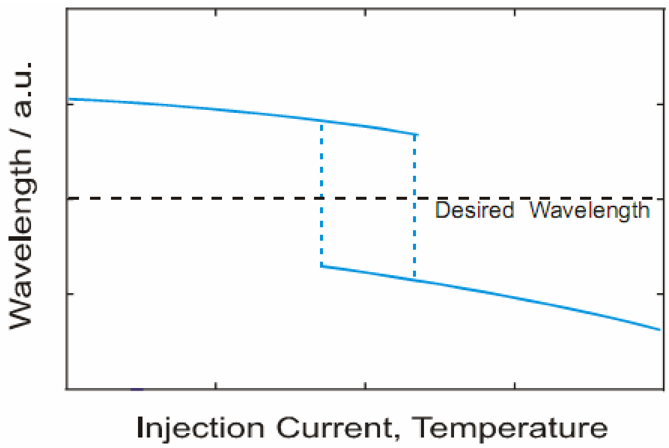

External resonator diode lasers

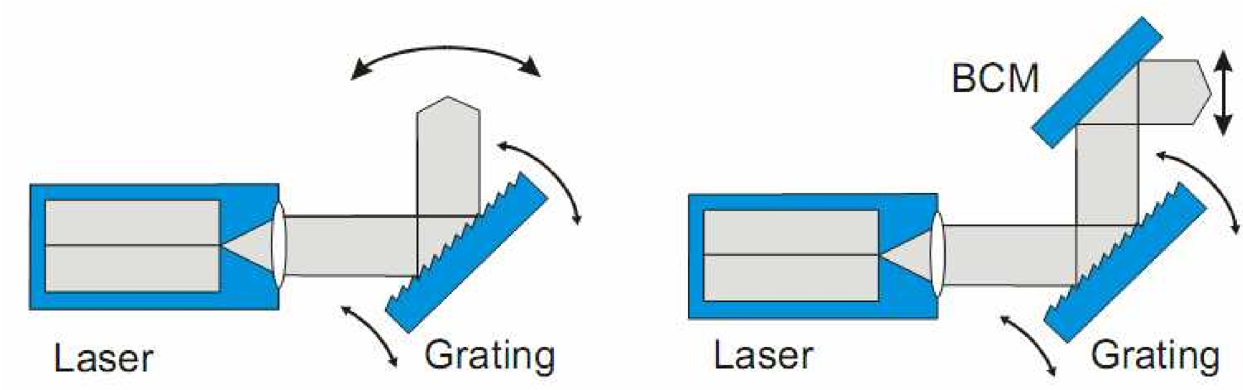

Fig.: Sacher Lasertechnik

Littrow configuration:

- tuning: grating rotation
- mode-hop free tuning range: typically 4-6 GHz
- beam steering may be avoided by using a beam-correction-mirror

External resonator diode lasers

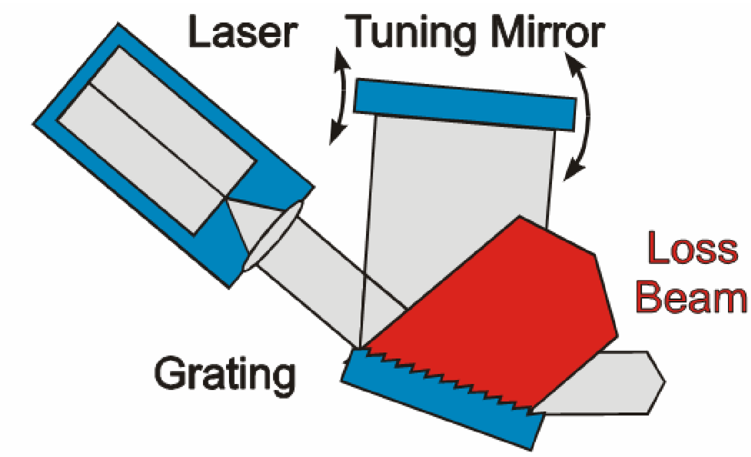

Fig.: Sacher Lasertechnik

Littman-Metcalf configuration:
- tuning: mirror rotation
- coupling can be controlled
- stable output direction
- higher losses

Construction

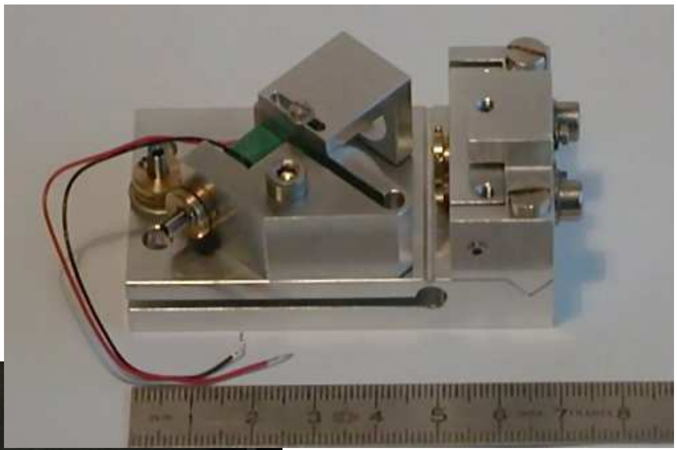

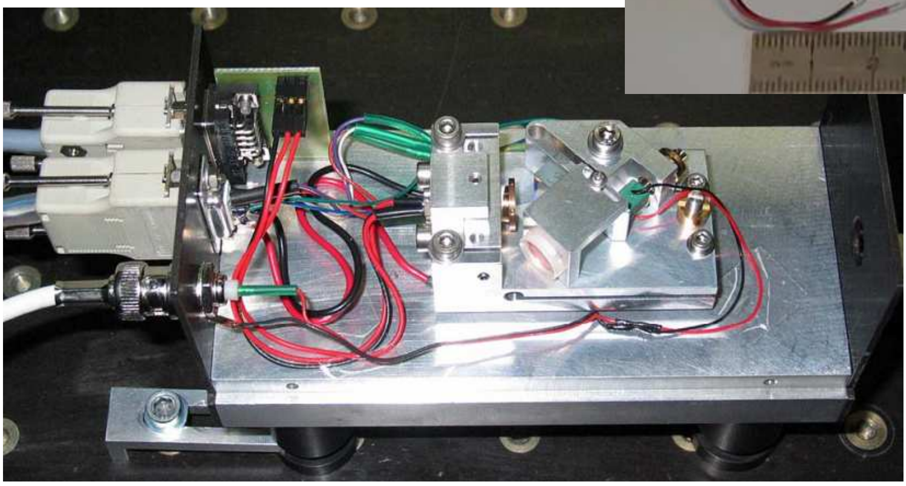

Comparison

	Littrow	Littman/Metcalf
	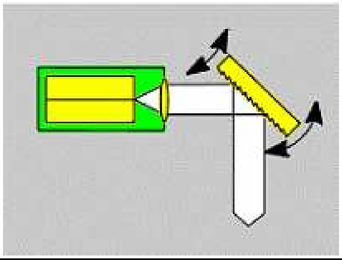	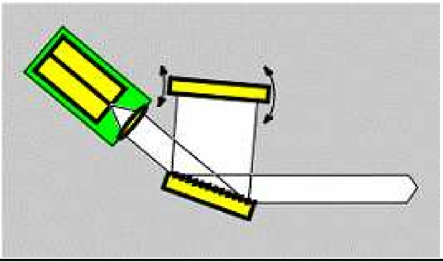
Output Power	5 … 100mW	3 … 30mW
Linewidth (50ms)	1 MHz	300 kHz
Linewidth (20s)	5MHz	2MHz
Fiber Coupling	Yes, w. beam correction mirror	Yes

Mode-hop free tuning

Problem

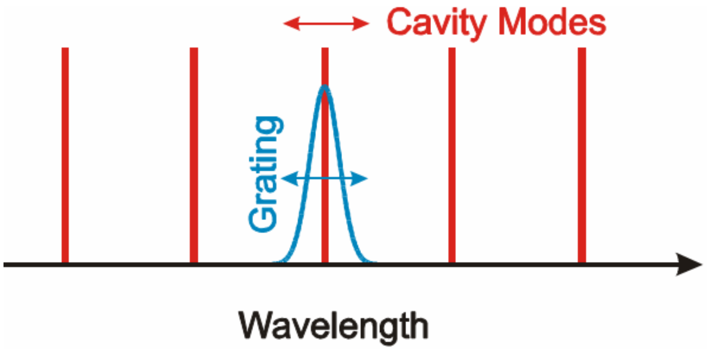

- Antireflection coating of the diode R = 5.10^{-4} .. 5.10^{-5} reasonable coupling of the laser diode
- Special geometry of the resonator

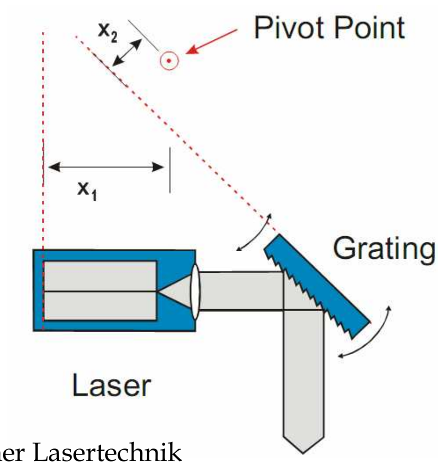

Fig.: Sacher Lasertechnik

Lasers: frequency stabilization

- side-of-fringe
  depends on amplitude,
  simple

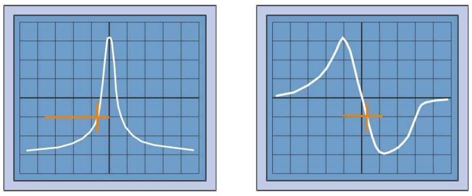

- top-of-fringe
  requires lock-in detection,
  more complicated

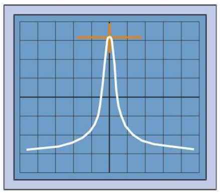

Lasers: frequency stabilization

Reference:

- External resonator
- Saturated absorption
- Polarization spectroscopy
- Atomic dichroism
  (Dichroic Atomic Vapor Laser Lock)
- Saturated dichroism
  (Doppler Free Dichroic Lock)

Saturated absorption

Saturated absorption locking scheme

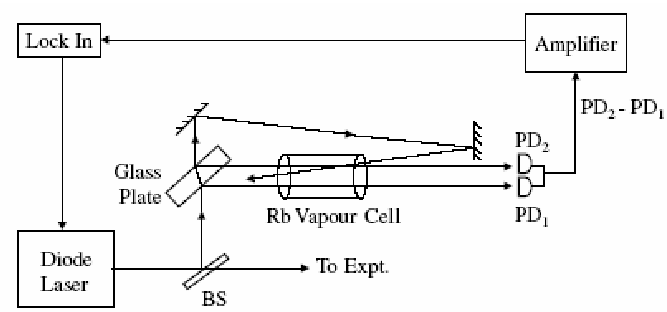

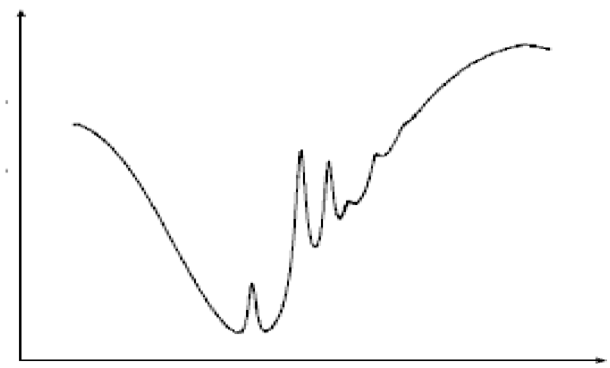

DAVLL

Fig.: J.Phys.B:At.Mol.Opt.Phys. 40 (2007)187–19

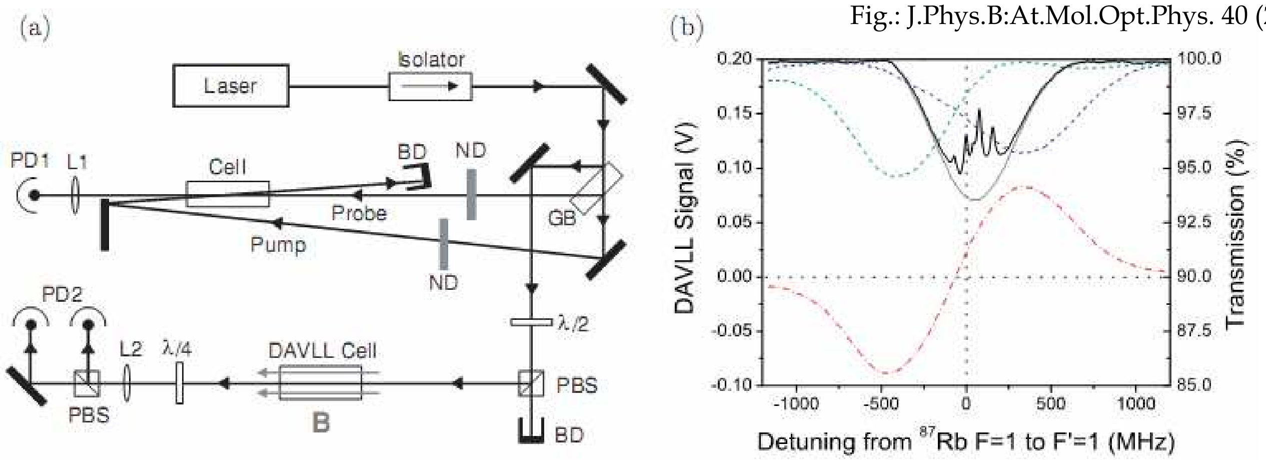

Differential absorption of two circular polarizations

Doppler broadened anti-symmetric curve:
no lock-in required
(poor absolute calibration)

Broad capture range

Shift of the locking point possible

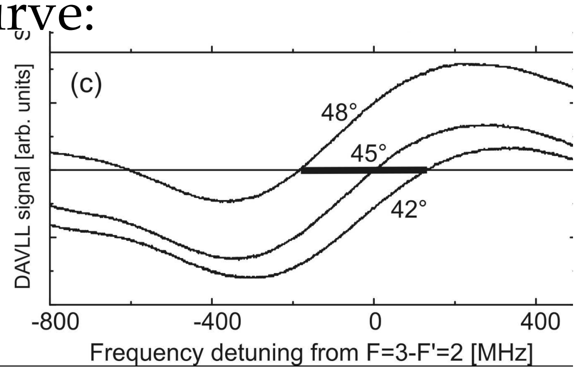

DFDL

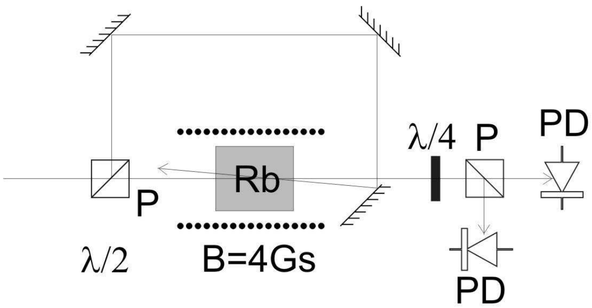

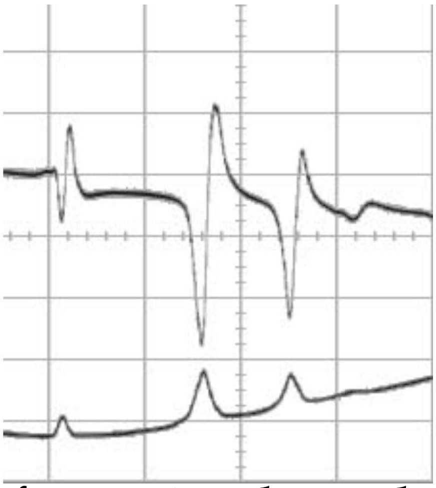

- Differential saturated absorption of two circular polarizations
- Doppler-free anti-symmetric curves: no lock-in required
- Better absolute calibration
- Small capture range
- Small shift of the locking point possible

G. Wąsik et al. Appl. Phys. B75, 613–619 (2002

Why fast modulation?

- Noise amplitude $\propto f^{-1}$
- Lock-in detection:
  shorter time constants → faster reaction of the controller
- Electro-Optic Modulators: up to GHz bandwidth

FM spectroscopy

Setup

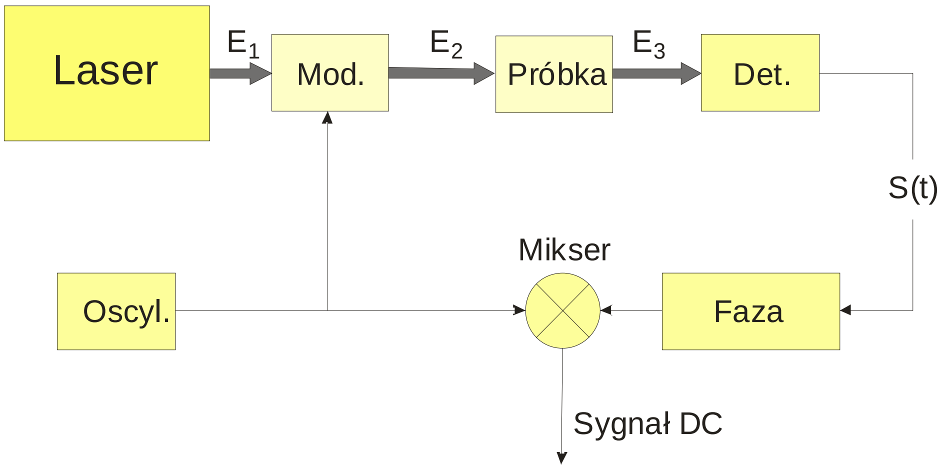

First application to optical range:

- G.C. Bjorklund, IBM Invention Disclosure, 1979, US Patent, 1981
- G.C. Bjorklund, Opt. Lett. **5**, 15 (1980),
- R.G.P. Drever, J.L. Hall, F.V. Kowalski, J. Hough, G.M.Ford, A.J. Munley

FM spectroscopy

Laser field behind the modulator:

$$E_2(t) = E_0\left\{-\frac{M}{2}\exp[i(\omega_C-\omega_m)t]+\exp(i\omega_C t)+\frac{M}{2}\exp[i(\omega_C+\omega_m)t]\right\}$$

Behind the sample an additional factor:

$$T_j = \exp(-\delta_j - i\phi_j);\quad \delta_j = \alpha_j L/2;\quad \phi_j = n_j L(\omega_C + j\omega_m)/c$$

$$E_3(t) = E_0\left\{-T_{-1}\frac{M}{2}\exp[i(\omega_C-\omega_m)t]+T_0\exp(i\omega_C t)+T_1\frac{M}{2}\exp[i(\omega_C+\omega_m)t]\right\}$$

Intensity measured by the detector:

$$I_3(t) = \frac{cE_0}{8\pi}e^{-2\delta_0}\left[1+(\delta_{-1}-\delta_1)M\cos\omega_m t+(\phi_1+\phi_{-1}-2\phi_0)M\sin\omega_m t\right]$$

FM spectroscopy – signal shape

Demodulated signal versus laser frequency at fixed ω_m

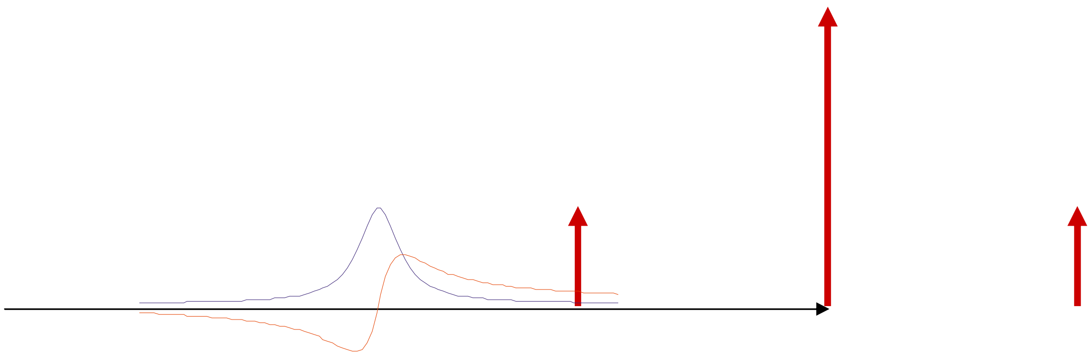

FM spectroscopy – signal shape

Demodulated signal versus laser frequency at fixed ω_m

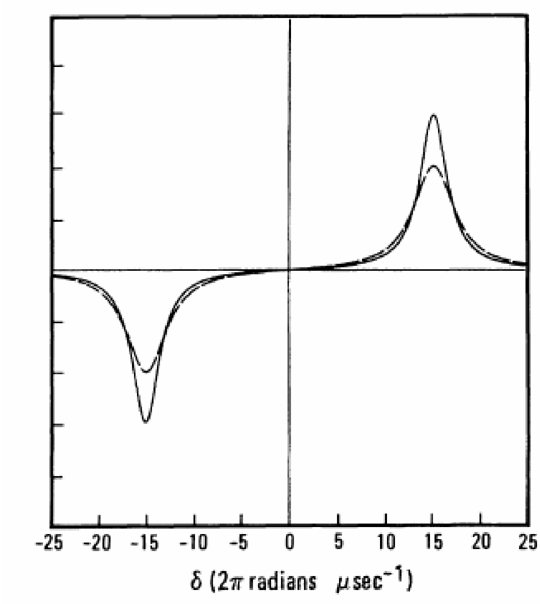

Absorption part

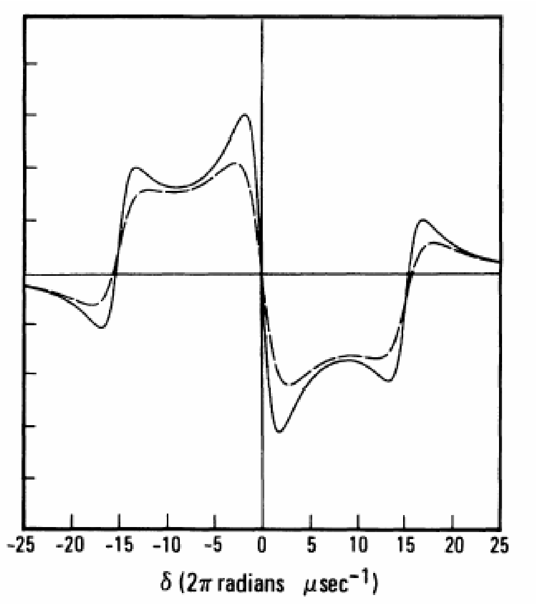

Dispersion part

Laser stabilization to F-P cavity

R.W.P. Drever, J.L. Hall, F.V. Kowalsky et al., Appl. Phys. B 31 (1983) 97 + R.V Pound earlier work on μ-waves

Now: „Pound-Drever-Hall stabilization method"

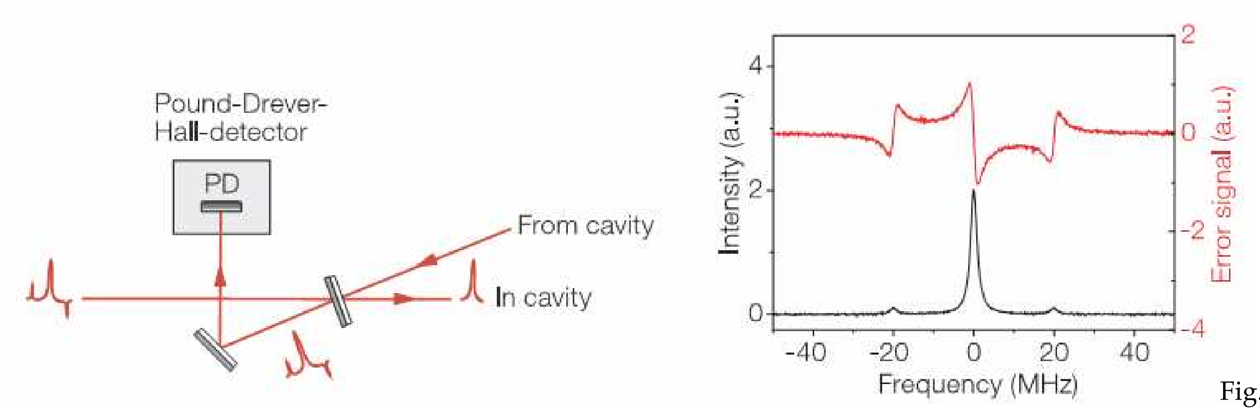

Fig.: Toptica

ω_m~10MHz: high enough for low noise, low enough for spectroscopy

Hansch-Couillaud method

T.W. Hänsch, B. Couillaud, Opt. Comm. 137 (1997) 295

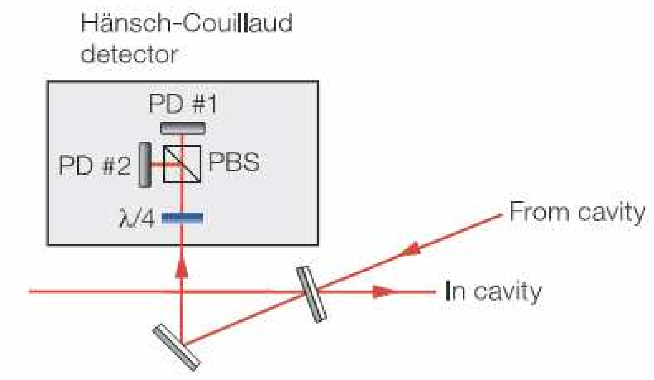

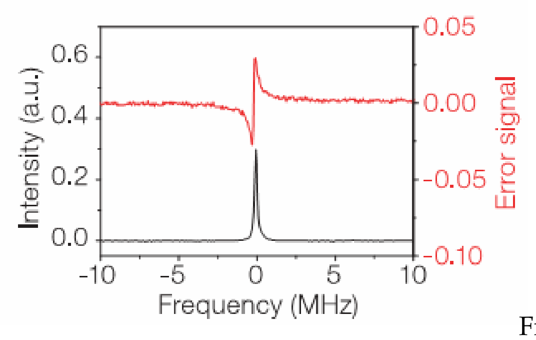

Fig.: Toptica

F-P cavity with polarization-dependent losses: Brewster plate, polarizer or a birefringent crystal,

Hansch-Couillaud method

Polarization components parallel & perp. to minimum loss direction:

$$E_{\parallel}^{(r)} = E_0 \cos\theta, \quad E_{\perp}^{(r)} = E_0 \sin\theta,$$

$$E_{\perp}^{(r)} = E_{\perp}^{(0)} r_1, \quad E_{\parallel}^{(r)} = E_{\parallel}^{(0)} \left(r_1 - \frac{t_1^2}{r_1} \frac{r e^{i\delta}}{1 - r e^{i\delta}} \right), \quad \delta = 2\Delta\omega L / c.$$

Perpendicular component – reflected at entrance window, no phase shift, serves as reference,
Parallel component – detuning-dependent phase shift,
Combined beam – elliptic polarization, except at resonance.
Difference signal of the photocurrents of the two detectors:

$$i_1 - i_2 \propto \left| E^{(0)} \right|^2 2 \cos\theta \sin\theta \frac{t_1^2 r^2 \sin\delta}{\left(1 - r^2\right)^2 + 4r^2 \sin^2 \delta / 2}$$

Comparison

Hänsch-Couillaud	Pound-Drever-Hall
Polarization sensitive stabilization	RF sideband modulation technique
Easier to implement	Adjustable locking range, defined by modulation frequency
No laser modulation required	Sideband modulation easily realized with diode lasers
Temperature and alignment sensitive	EOM / AOM needed for non-diode lasers

Laser beam shaping

- Required shape: pure TEM_{00} mode
  - ❖spatial filtering with pinholes
  - ❖filtering by a single-mode optical fiber
- Power loss
- Possibility of separation of laser table from experiment table
- Polarization maintaining fibers!

Acousto-optic modulators

- Laser beam diffracted on an acoustic wave (elastooptic effect),
- Glass, quartz, lead molybdate, tellurium oxide
- Running acoustic wave,
- Acoustic velocity ~5 km/sec,
- Transducer frequency 40–300 MHz.

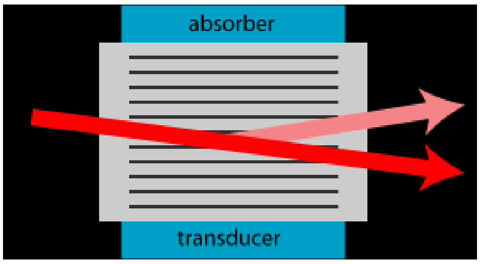

beam deflection, $\varphi(f_{AOM})$

intensity control, $I_{\pm1}(P_{rf})$

frequency change: $f_{out} = f_{in} + f_{AOM}$

Acousto-optic modulators

- Acousto-optic **modulators** are used to vary and control laser beam intensity.
- A **frequency shifter** uses the shift inherent in the acousto-optic interaction to up- or down-shift a laser's frequency.
- A **deflector** is used to scan a laser beam over a range of angles. The angle of the first order output beam is directly linked to the RF frequency. By varying the frequency, the output laser beam angle is modified.

Acousto-optic modulators

Example specifications: ISOMET model 1206C

Spectral Range:	.442-> 1.5μm*
Standard Operating Wavelengths:	442nm, 488-633nm
Interaction Medium:	Lead Molybdate (PbMo04)
Acoustic Velocity:	3.63mm/μs
Active Aperture:	1mm
Centre Frequency (CF):	110MHz
RF Bandwidth:	50MHz
Input Impedance:	50Ω
VSWR:	<1.5:1 @ 110MHz
DC Contrast Ratio:	>1000:1 min (2000:1 typical)

PERFORMANCE vs. WAVELENGTH

Wavelength (nm):	442	488	515	633
RF Drive Power	<0.4	<0.5	<0.5	<1.0
Bragg angle (mr):	6.7	7.4	7.8	9.6
Beam Separation (mr)	13.4	14.8	15.6	19.2
Static Insertion Loss:	<10	<5	<3	<3

PERFORMANCE vs. BEAM DIAMETER

Beam Diameter (mm):	1.0	0.34	0.2	0.084
Rise Time (ns):	180	60	35	15
Video Bandwidth (MHz):	2	6	10	25
Deflection Efficiency (%):	>85	>85	>80	>60
T Δf Product:	16	N/A	N/A	N/A

AOM tips & tricks

- Double pass: frequency shift scan without beam deflection

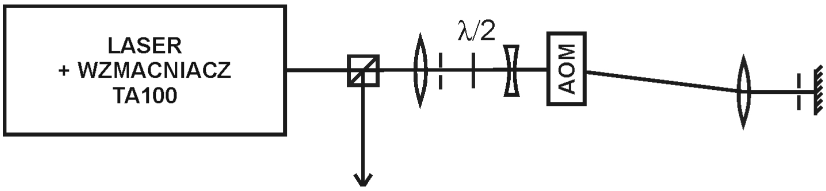

- Caution: birefringence!
- Double pass, single frequency shift
- Drivers: VCO, DDS

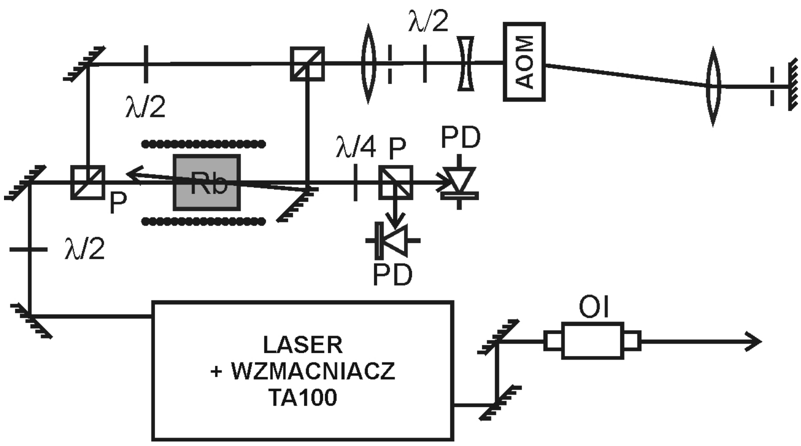

Electro-optic modulators

- Amplitude & phase modulators
- Frequency up to GHz
- For Pound-Drever-Hall stabilization 10-20 MHz
- Broadband or resonant modulators

Atom sources

- Evaporative sources
- Atomic beam oven
- High flux sources
- Dispenser
- LIAD

Atomic beam oven

- Heated container + output opening
  Example for Sr: 200 tubes of 8-mm length and 200-µm diameter for transverse velocity selection.

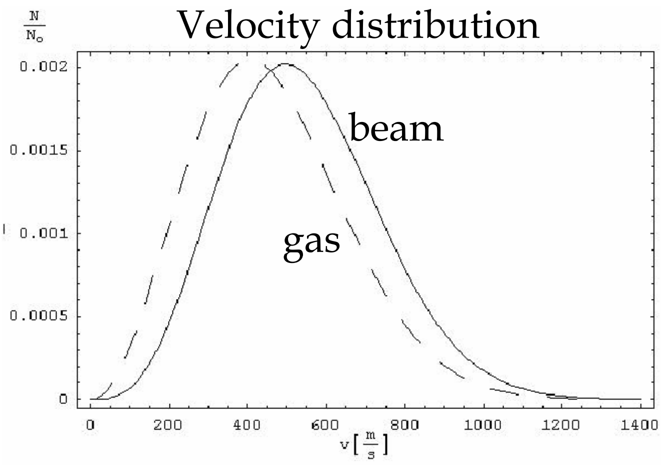

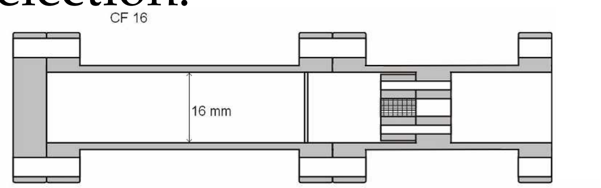

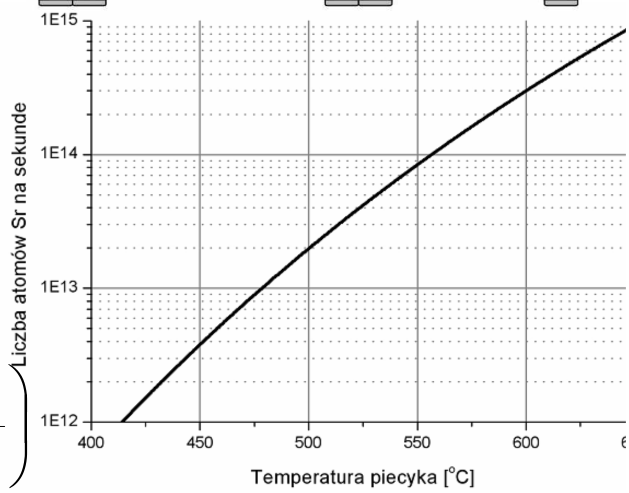

$$f^{beam}(v) \propto v^3 \exp\left(-\frac{v^2}{2u^2}\right), \qquad f^{gas} \propto v^2 \exp\left(-\frac{v^2}{2u^2}\right)$$

High-flux effusive beam

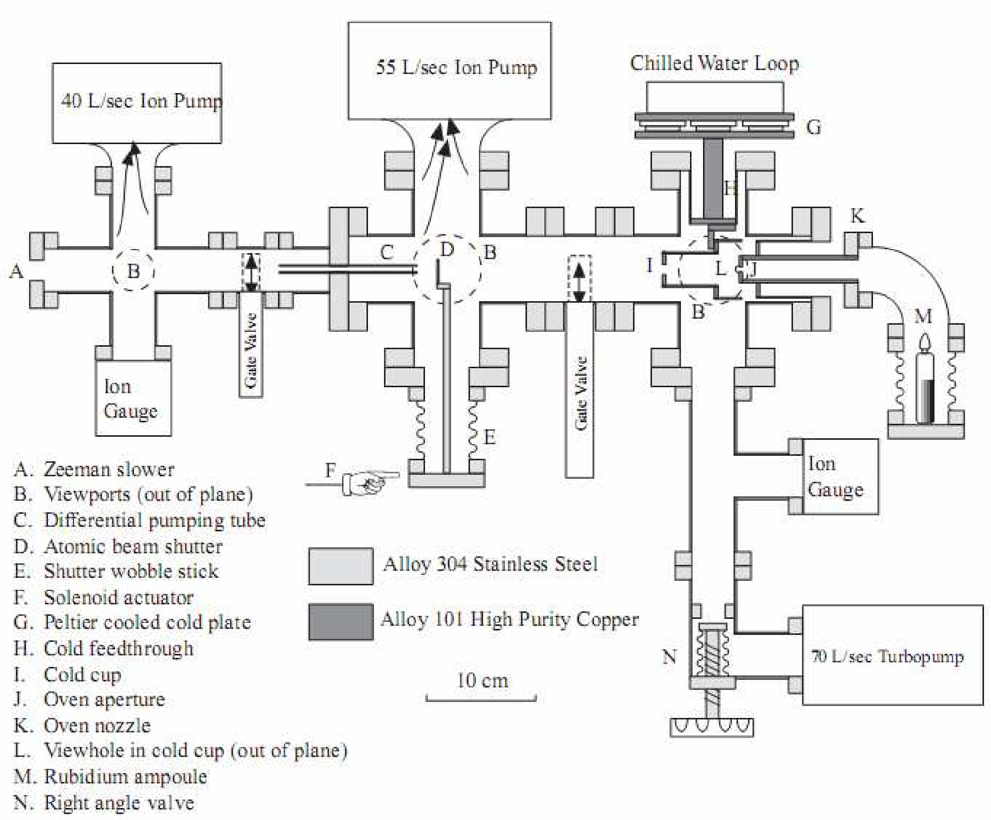

Oven temp 110–150°C
$p_{Rb} \sim 0.5$ mtorr
hole (J) dia. 5 mm
hole (I): 7.1 mm dia.
flux ~ 10^{11} atoms/s.
cold cup temp -30°C
capture 99.3% of atoms
$p_{Rb} \approx 2.5 \times 10^{-10}$ torr.

E. Streed Thesis MIT 2006

Candlestick source

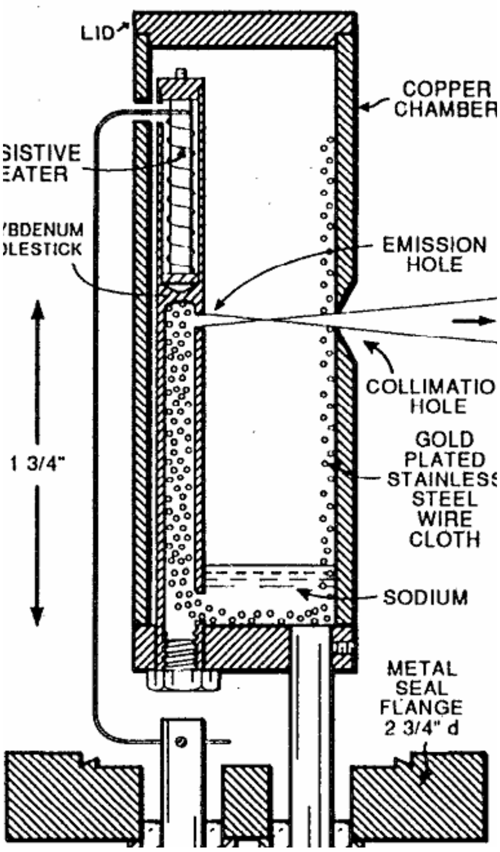

Na source:
emission point temp. 350ºC:
total flux 10^{18} at/s
Rb source:
emission hole 2 mm
collimation hole 2mm
dist. 2 cm
divergence π/50 rad
emission point temp. 160ºC:
total flux 1.2×10^{14} at/s
mean velocity 400 m/s

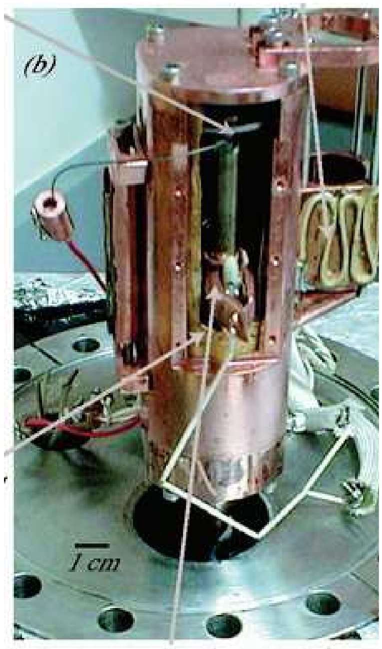

L.V. Hau and J.A. Golovchenko
Rev. Sci. Instrum. 65 (12), December 1994

Candlestick source

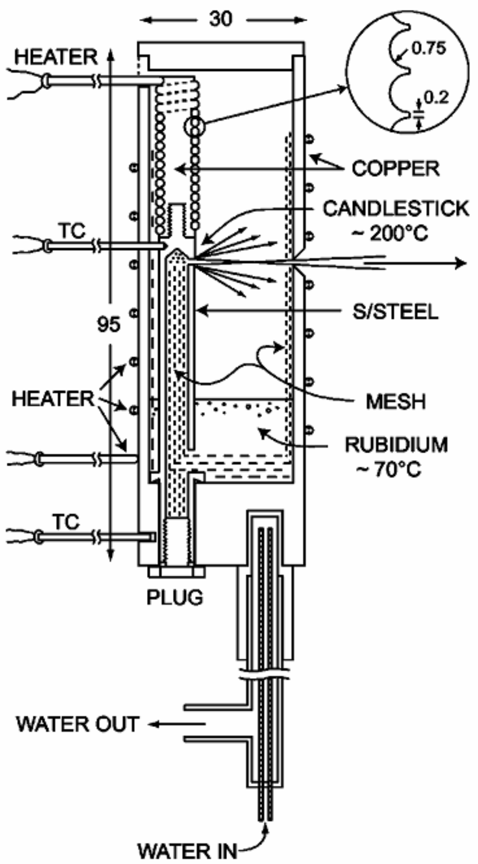

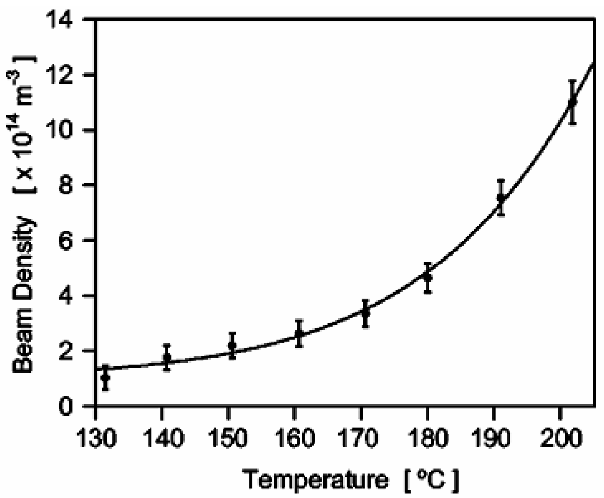

Atomic density in the beam 35 cm from the sour

M Walkiewicz et al.
Rev.Sci.Instrum.,Vol.71,No.9,September2000

Alkali Metal Dispensers

SAES Getters S.p.A.

Cs, Na, K, Rb, Li

alkali metal chromate + reducing agent (Zr-Al getter)

heating by electric current:
5 A for 650°C

easy handling and vacuum installation, fast response

a current burst at the beginning to break the oxide layer

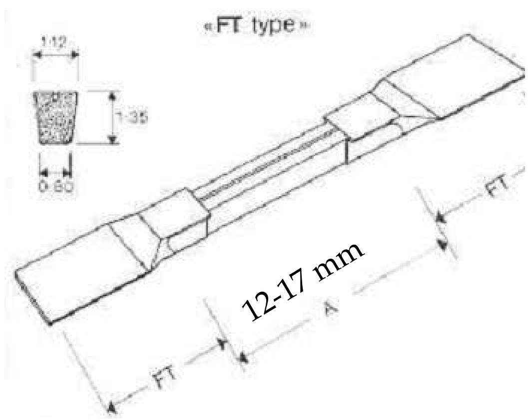

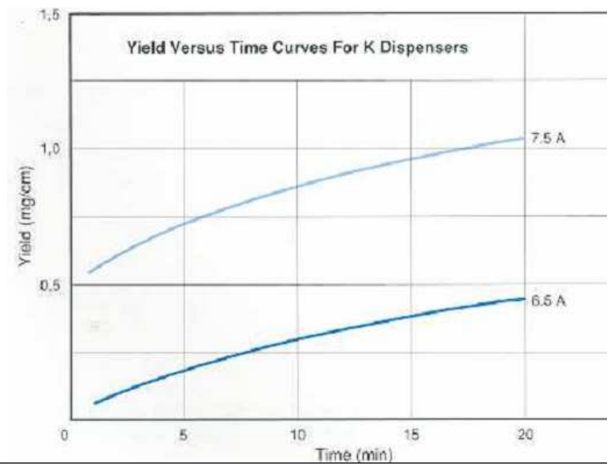

Vacuum apparatus

- Different requirements for atom collection and experiment (e.g. BEC) areas,
- Pressure in atom collection chamber ~10^{-8} mbar (alkali metal dispensers)
- Pressure in experimental chamber <10^{-10} mbar
- Two chambers should be separated and differentially pumped

Vacuum chambers

- Materials:
  - stainless steel (304, 316 type),
  - quartz,
  - gaskets: copper, indium wire,
- Flanges and fittings CF type

ISO description	Nominal ID	Outside diameter
DN16CF	19	34 (1 1/3″)
DN40CF	38	70 (2 ¾″)
DN63CF	63	114 (4 ½″)
DN100CF	100	152 (6″)
DN160CF	150	203 (8″)

Vacuum pumps

- Ion pump
- Ti sublimation pump
- NEG (Zr-V-Fe or Ti-V getter alloys)
- Turbopump

Vacuum preparation

1. wash parts in ultrasonic cleaner: alkaline detergent, trichloroethylene, alkaline degreaser,
2. rinse in demineralised water,
3. dry in hot air
4. close chamber: all screws silvered or coated with molybdenum disulphide (MoS_2) dry lubricant
5. pump the chamber to ~10^{-8} mbar: turbomolecular pump + oil-free roughing pump
6. vacuum bake

Vacuum baking

1. cover the glass cells,
2. install heating tapes and thermocouples,
3. raise the temperature to 300°C (not faster than 50°C/h) homogeneous heating (diff. < 30°C),
4. heat also metal dispensers and Ti wires in sublimation pump,
5. outgass dispensers and Ti wires,
6. bake turbo pump and ion pump,
7. bake for 12 h with turbo pump on,
8. close the turbo pump valve,

Vacuum baking cont.

9. bake for 48h with ion pump on,
10. cool the apparatus in 6–8 h,
11. end pressure < 10^{-10} mbar.

Vacuum pumping

- molecular flows if
  mean free path > chamber size
  i.e. pressure × size < 10^{-2} Pa m
- pump speed S: volumetric flow (l/s, m^3/h, cfm)
- pump throughput T: measure of the *quantity* of gas the pump can remove (torr.liter/sec, Pa m^3/s = W)
- effective pumping speed EPS: combination of conductance and pumping speed

Vacuum pumping

$$T = S \cdot p$$

flow in the connecting tube depends on the conductance and pressure diff.:

$$T = C\,(p_c - p_p)$$

no losses and leaks

$$\frac{1}{EPS} = \frac{1}{C} + \frac{1}{S} \quad \text{or} \quad EPS = \frac{S}{1 + S/C}$$

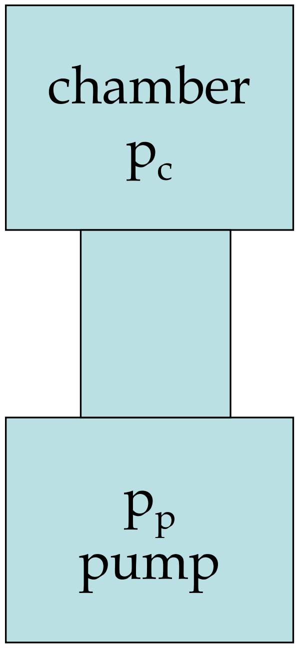

Conductance

- Circular opening: C[l/s] = 37 r^2 [cm^2]
- Circular tube: C[l/s] = r^3[cm^3]/l[m]

Example:

pump S = 300 l/s

tubing section l = 10 cm, Ø = 4 cm, C_t = 80 l/s

valve NW40 C_v = 45 l/s

EPS = 26 l/s (only!!!)

Moreover: p_c/p_p = S/EPS → p_c 10 times more than in pump

Construction rules

- It’s easy to spoil conductance,
- Weakest element decisive for total conductance,
- All connections should be short and wide
- Best: pump directly connected to chamber
- Optical acces requirements, magnetic field etc. dictate non-perfect solutions

Magnetic fields

- Homogeneous fields: Helmholtz coils
- Quadrupole fields (MOT, traps)
- Zeeman slower solenoid

Equations

Magnetic field of a coil: radius R, axis OZ, position z=A

$$B_z = \frac{\mu I}{2\pi} \frac{1}{[(R+\rho)^2 + (z-A)^2]^{1/2}} \times \left[K(k^2) + \frac{R^2 - \rho^2 - (z-A)^2}{(R-\rho)^2 + (z-A)^2} E(k^2) \right],$$

$$B_\rho = \frac{\mu I}{2\pi\rho} \frac{z-A}{[(R+\rho)^2 + (z-A)^2]^{1/2}} \times \left[-K(k^2) + \frac{R^2 + \rho^2 + (z-A)^2}{(R-\rho)^2 + (z-A)^2} E(k^2) \right],$$

SI units (A,m,T):
$\mu = 4\pi\ 10^7$
mixed units (A,cm,G)
$\mu = 4\pi\ /10$

argument of the complete eliptic integrals K, E(z)

$$k^2 = \frac{4R\rho}{(R+\rho)^2 + (z-A)^2}.$$

Equations

Magnetic field of a wire parallel to z axis at cylindrical coordinates ρ=S, ϕ=α:

$$B_z = 0,$$

$$B_\rho = \frac{\mu I}{2\pi} \frac{S \sin(\phi - \alpha)}{[S^2 + \rho^2 - 2S\rho \cos(\phi - \alpha)]},$$

$$B_\phi = \frac{\mu I}{2\pi} \frac{S \cos(\phi - \alpha) - \rho}{[S^2 + \rho^2 - 2S\rho \cos(\phi - \alpha)]}.$$

Polynomial expansion

Single coil at z=0

$$B_z(z,\rho=0)=\frac{\mu I}{2R}\left[1-\frac{3z^2}{2R^2}+\frac{15z^4}{8R^4}+\cdots\right]$$

Two coils at z=±A

$$B_z(z,\rho=0)=\frac{\mu I R^2}{(R^2+A^2)^{3/2}}$$

$$\times\left[1+\frac{3z^2(4A^2-R^2)}{2(A^2+R^2)^2}\right.$$

$$\left.+\frac{15z^4(R^4-12A^2R^2+8A^4)}{8(A^2+R^2)^4}+\cdots\right]$$

Helmholtz config. for 2A=R: maximum field uniformity

Magnetic traps

Potential:

$$E_{pot} = -\boldsymbol{\mu} \cdot \mathbf{B} = -\mu_B \, g_F \, m_F \, B$$

Inhomogeneous field: Stern-Gerlach force,
no field maximum possible (Earnshaw theorem)
trap for „low-field-seeking states"

Magnetic moment follows the field direction if its orientation does not change too fast (adiabatic criterion)

$$\mathbf{v} \cdot \nabla \left(\frac{\mathbf{B}}{B} \right) << \omega_L$$

Magnetic traps

Quadrupole trap (W. Paul, W. Phillips):

two coils with opposed equal currents

linear potential – better trapping,

but at minimum B = 0: Majorana spin flips

Threshold values of |B| along z and ρ equal if A/R = 0.63.

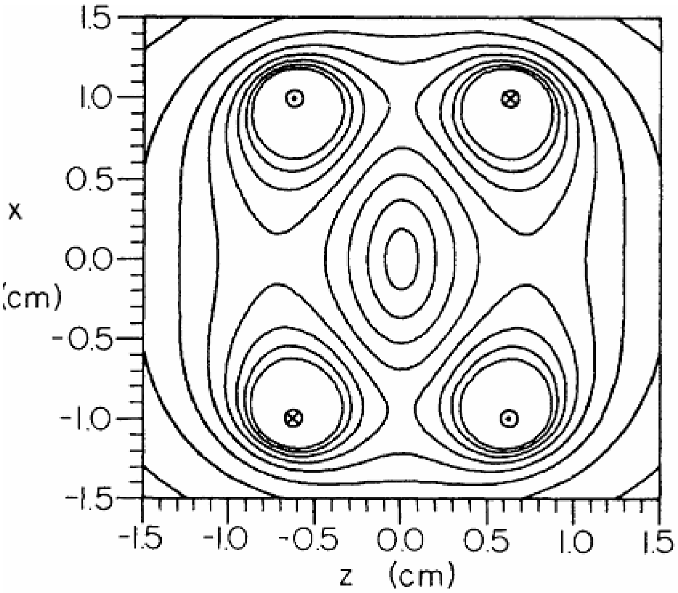

T. Bergeman et al. PRA 35, 1535 (1987)

Magnetic traps

Time-averaged Orbiting Potential (TOP)

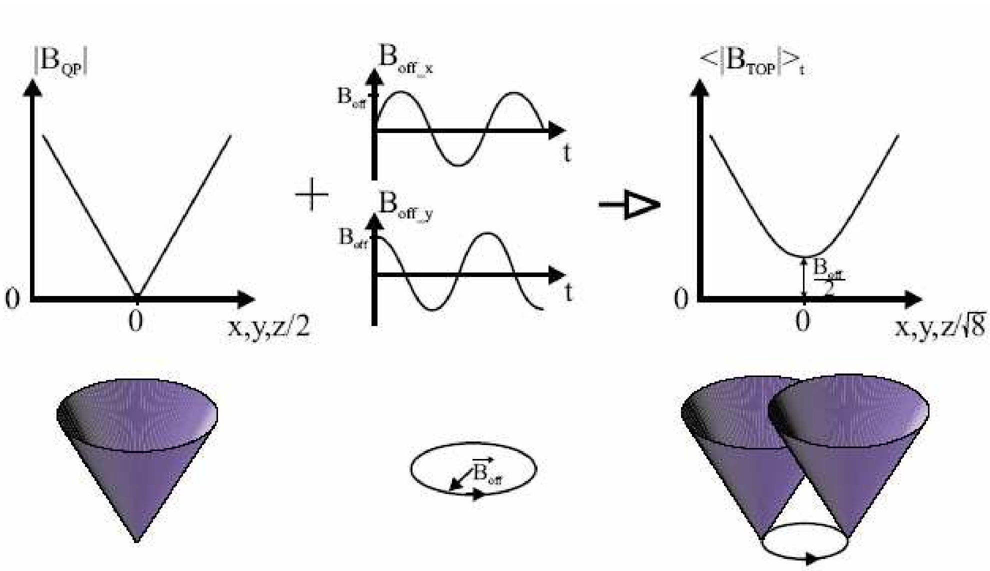

Joffe trap

Four conducting bars — quadrupole radial field
+ coils on axis (distance > Helmholtz coils) — axial field with a minimum
+ homogeneous offset field

Total field:

$$\mathbf{B}(\mathbf{r}) = B_0 \begin{pmatrix} 0 \\ 0 \\ 1 \end{pmatrix} + B' \begin{pmatrix} x \\ -y \\ 0 \end{pmatrix} + \frac{B''}{2} \begin{pmatrix} -xz \\ -yz \\ z^2 - \frac{1}{2}(x^2 + y^2) \end{pmatrix}$$

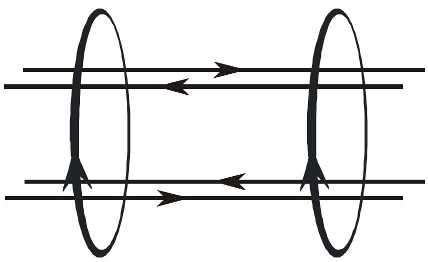

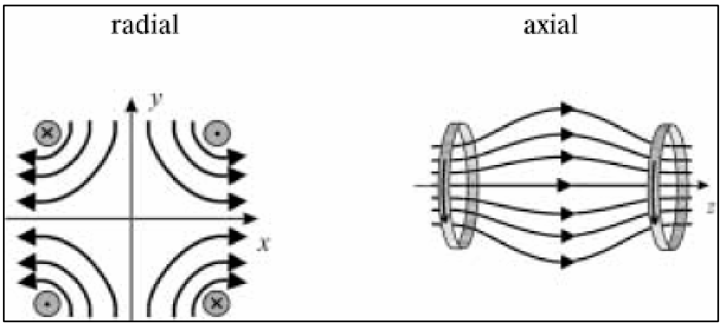

Joffe trap

Total field:

$$\mathbf{B}(\mathbf{r}) = B_0 \begin{pmatrix} 0 \\ 0 \\ 1 \end{pmatrix} + B' \begin{pmatrix} x \\ -y \\ 0 \end{pmatrix} + \frac{B''}{2} \begin{pmatrix} -xz \\ -yz \\ z^2 - \frac{1}{2}(x^2 + y^2) \end{pmatrix}$$

Harmonic potential close to trap center

$$U_{\text{harm}} = g_F m_F \mu_B \left[B_0 + \frac{1}{2}\left(\frac{B'^2}{B_0} - \frac{B''}{2}\right)(x^2 + y^2) + \frac{1}{2}B'' z^2 \right]$$

Oscillation frequencies:

$$\omega_\rho = \sqrt{\frac{g_F m_F \mu_B}{m}\left(\frac{B'^2}{B_0} - \frac{B''}{2}\right)} = \sqrt{\frac{g_F m_F \mu_B}{m} B''_\rho}$$

$$\omega_z = \sqrt{\frac{g_F m_F \mu_B}{m} B''}$$

Magnetic trap

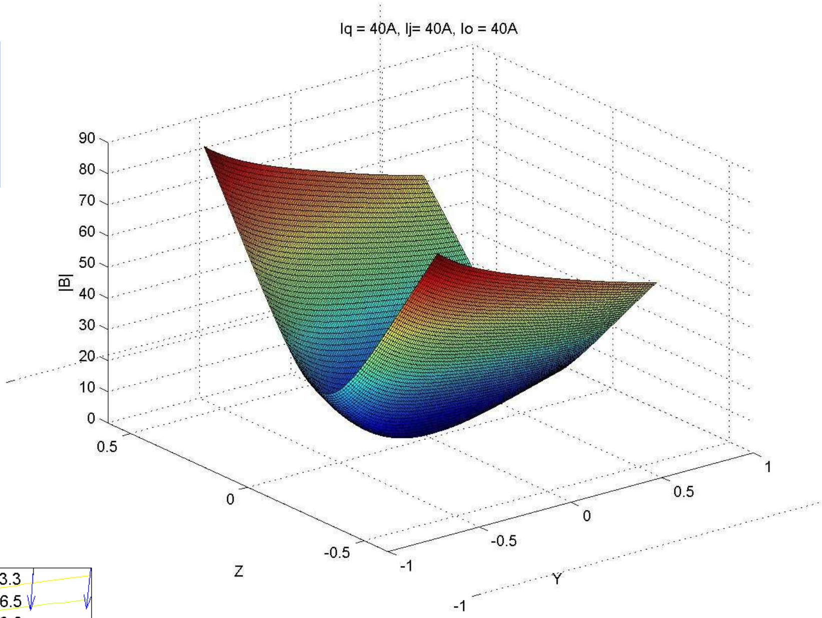

Field distribution

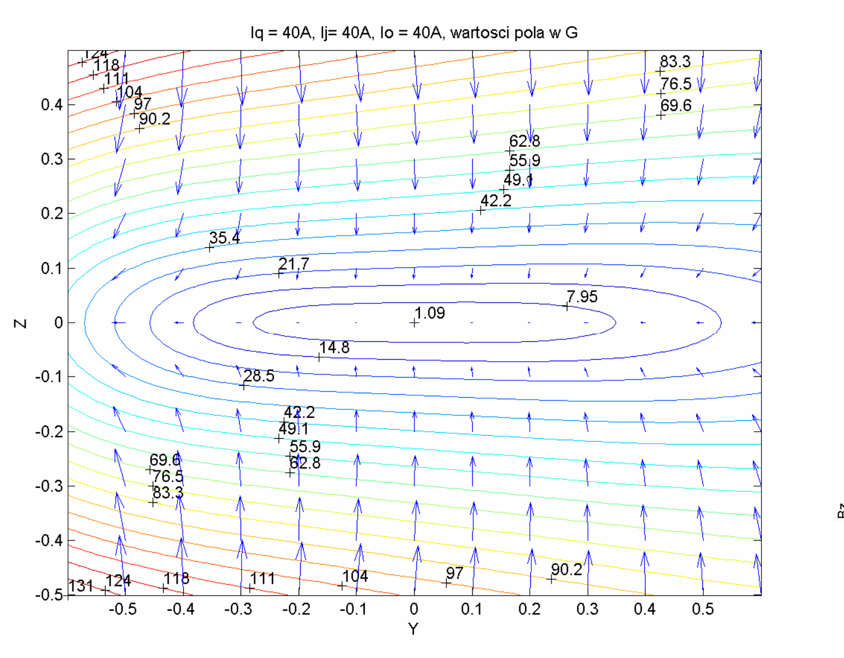

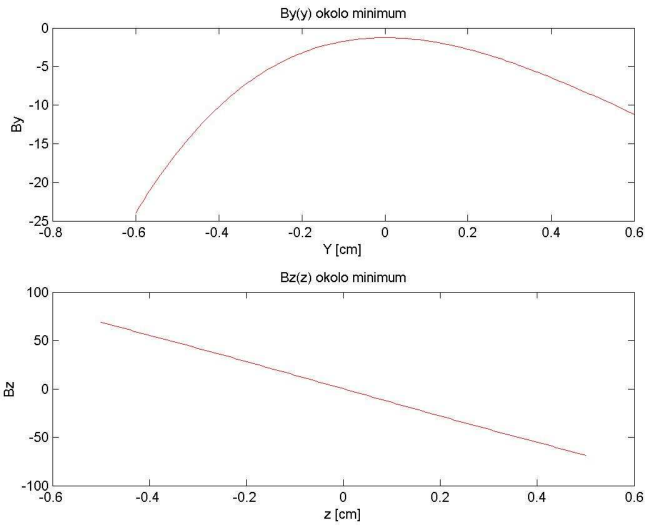

Magnetic trap

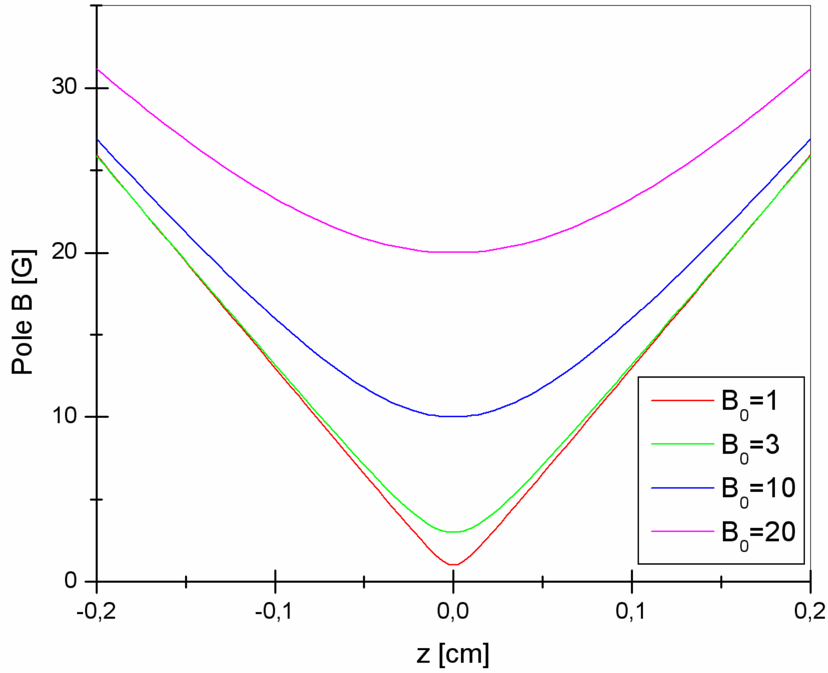

B Field along the Z axis for different offset field values

Harmonic range limited:

$$T_{lin} \simeq \frac{m_F g_F \mu_B}{k_B} B_0$$

Magnetic trap

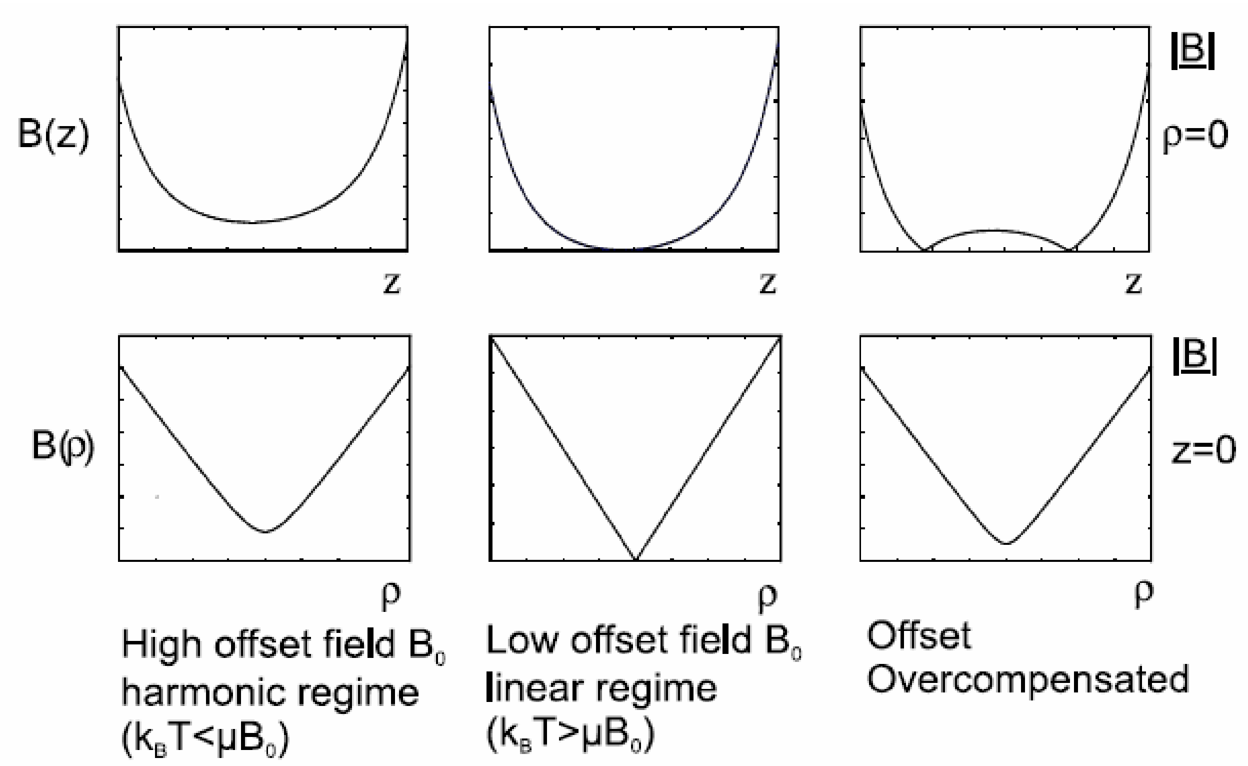

QUIC

QuadrUpole-Joffe Configuration

T. Esslinger, I. Bloch, and T.W. Hansch. Phys. Rev. A, **58**, *R2664 (1998)*

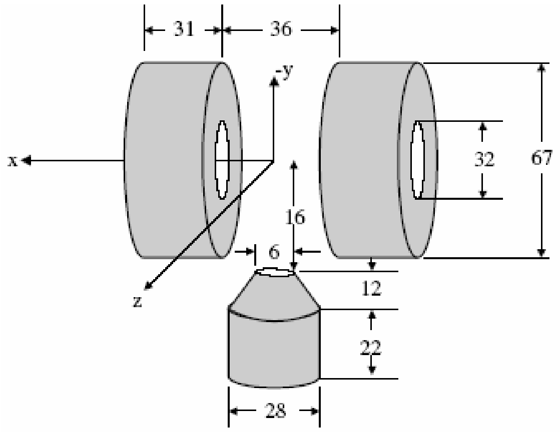

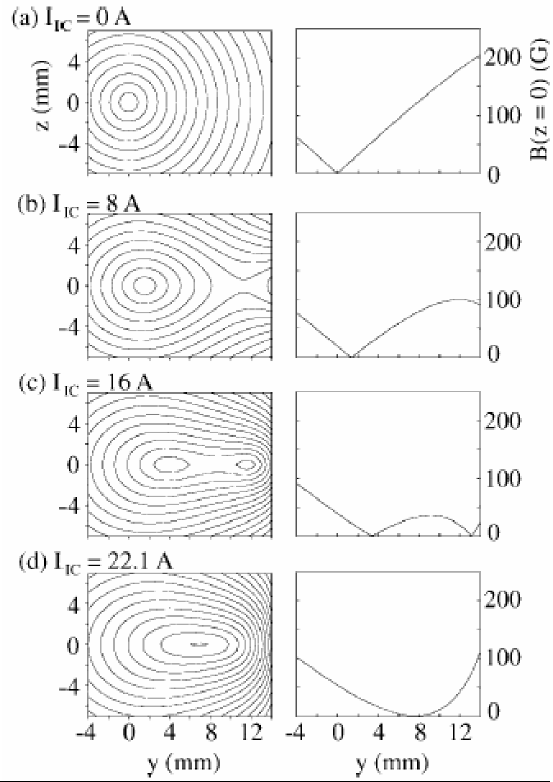

Position of the field minimum shifts with the Joffe coil current increase

Another version of QUIC

Three identical coils:

- quadrupole + Joffe coil
- field minimum remains in the same position,
- high value of minimum field.

Additional Helmholtz coils:

- offset field

Dalibard, 2001

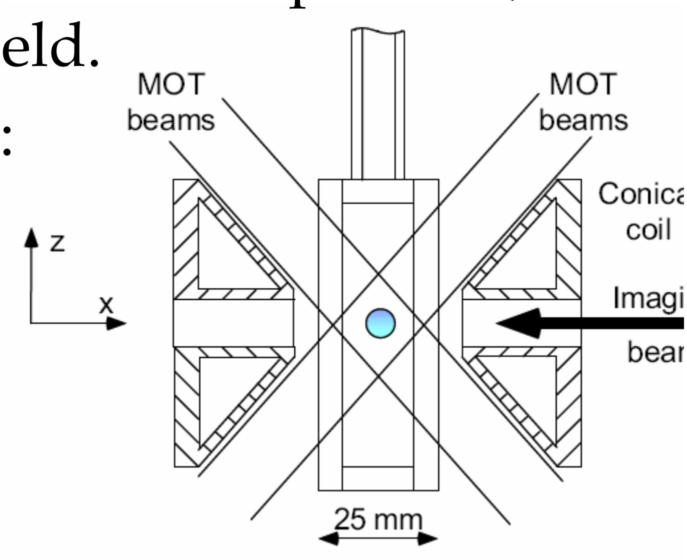

Magnetic trap

coils (MT) water cooled
(40 A, Ø = 1 mm)

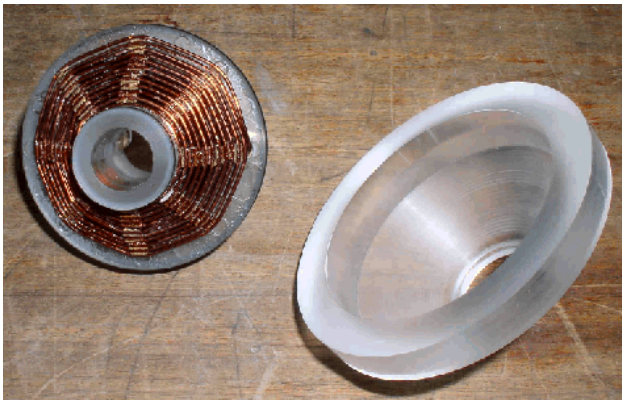

offset coils – Cu tubing

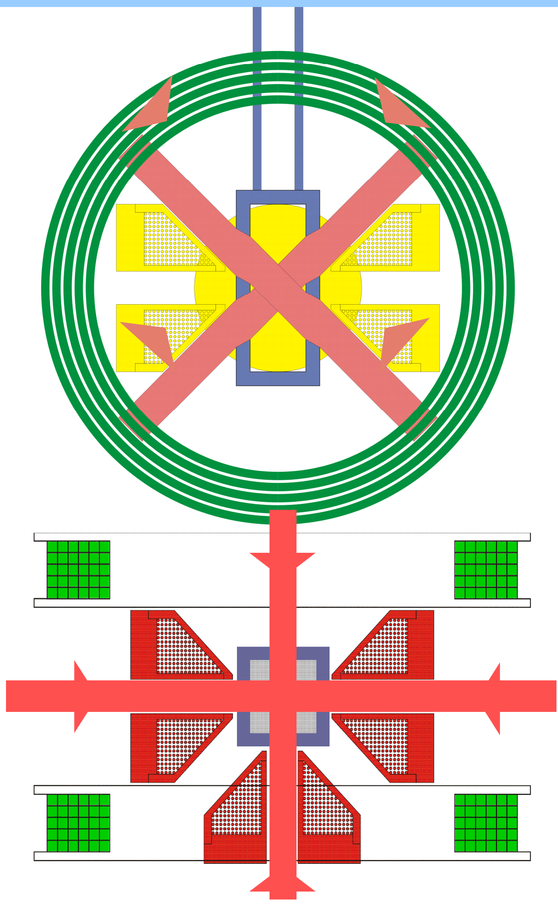

Magnetic coils

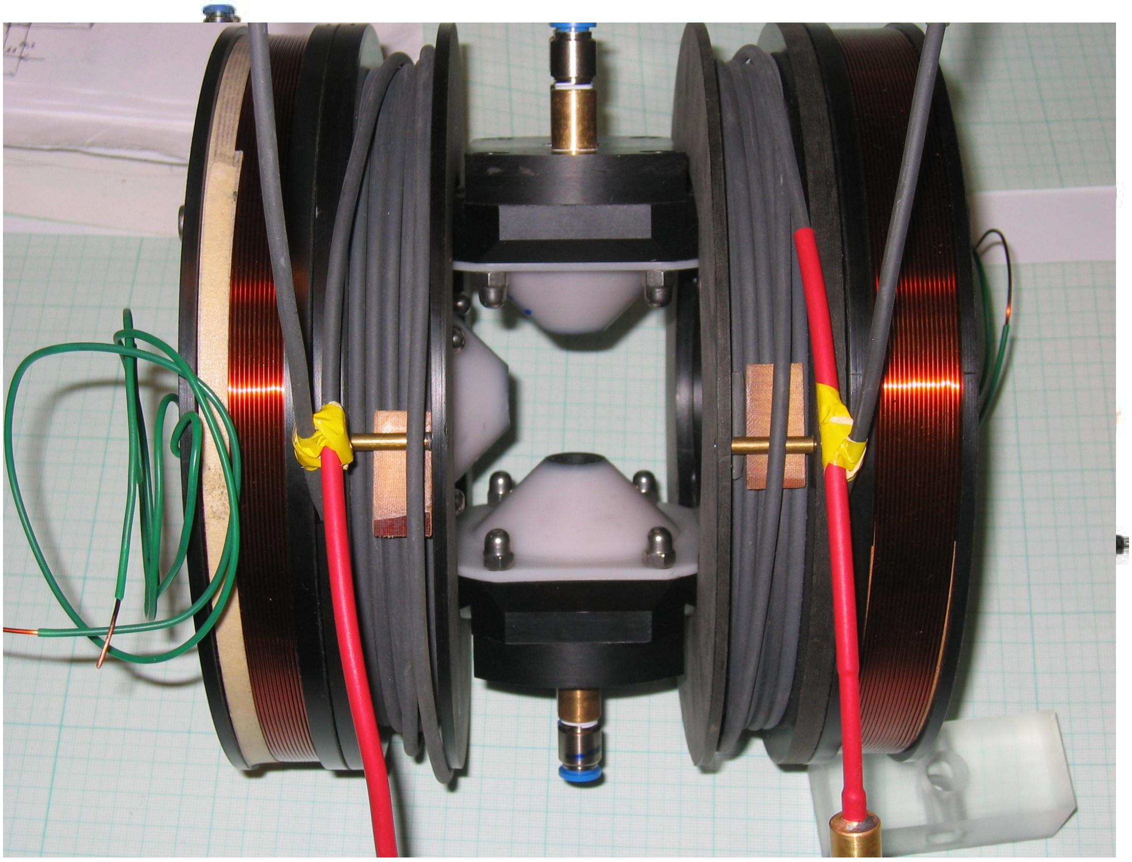

Surface traps (atom chips)

R. Folman et al. MICROSCOPIC ATOM OPTICS: FROM WIRES TO AN ATOM CHIP, Adv.in At., Mol. & Opt. Phys. 48

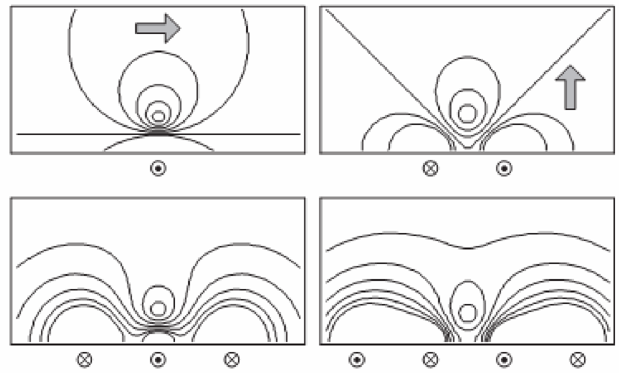

Potential for magnetic guides

Surface traps (atom chips)

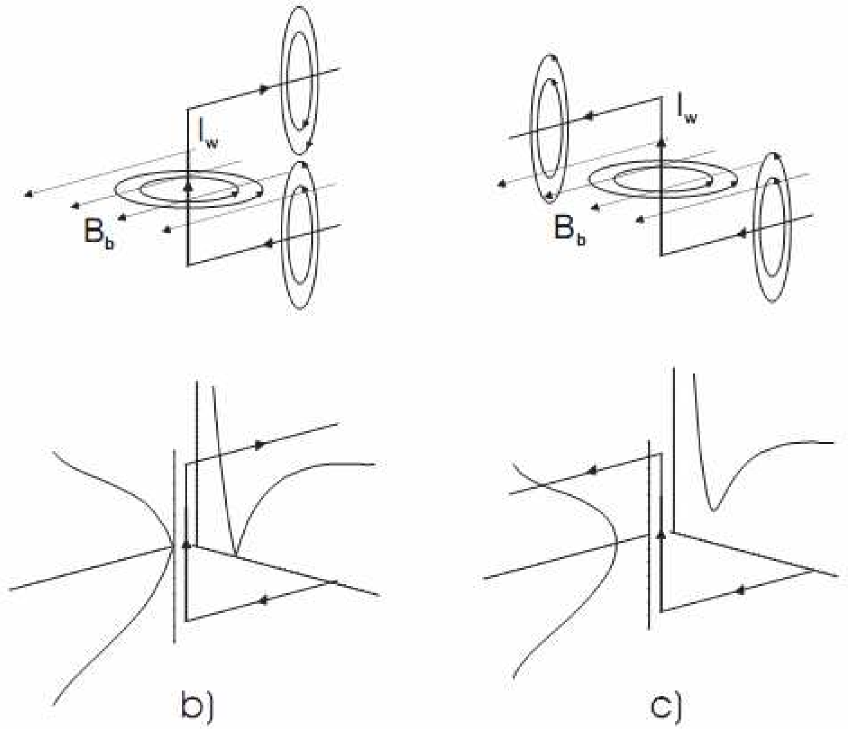

b) U-wire trap:
3-D quadrupole field with a zero in the trapping center,
c) Z-wire trap:
Ioffe–Pritchard type trap

radial and axial trapping potential

Surface traps (atom chips)

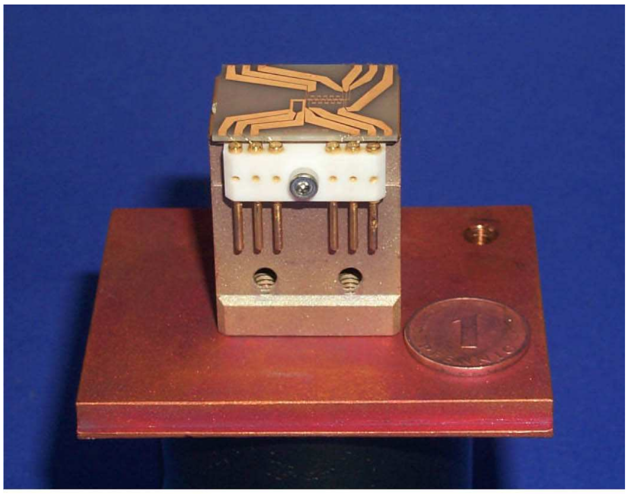

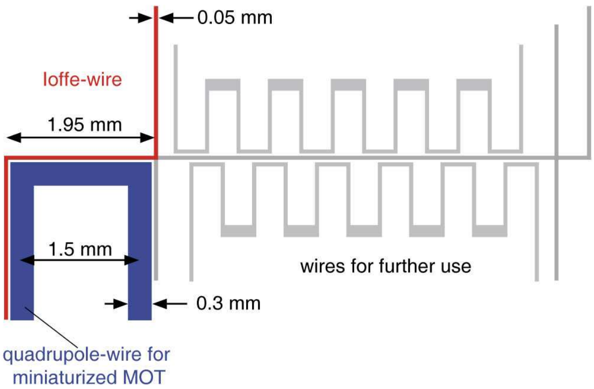

Trap and magnetic ‘conveyor belt’:
MPQ Garching
87Rb
Atom number in BEC: 6000
Collecting time: 8s
Cooling time 2,1s
Current 2A

Zeeman slower solenoid

- Local magnetic fields compensate Doppler shift
- Simplest case: constant deceleration assumed, no laser detuning
- $B \propto z^{1/2}$
- Inconvenient:
  high fields required
  difficult to control end velocity
- Better:
  detune the laser

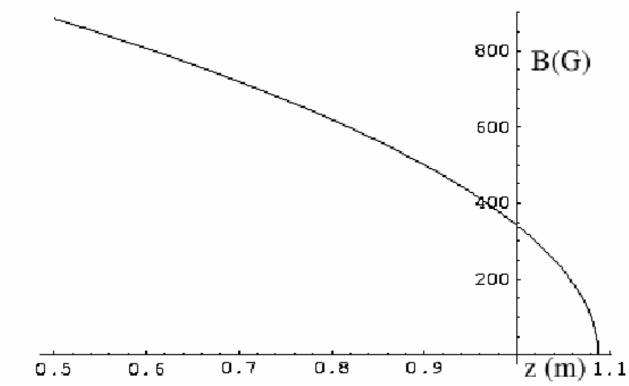

Zeeman slower solenoid

- Non maximum deceleration assumed $a=\varepsilon a_{max}$
- Big detuning of the laser beam
- Magnetic shields for better field confinement
- Complicated winding pattern

$$B(z)=\frac{\hbar}{\mu_B}\left(-\delta_o-kv(z)+\frac{\Gamma}{2}\sqrt{(1+S(z))\frac{1-\epsilon}{\epsilon}}\right).$$

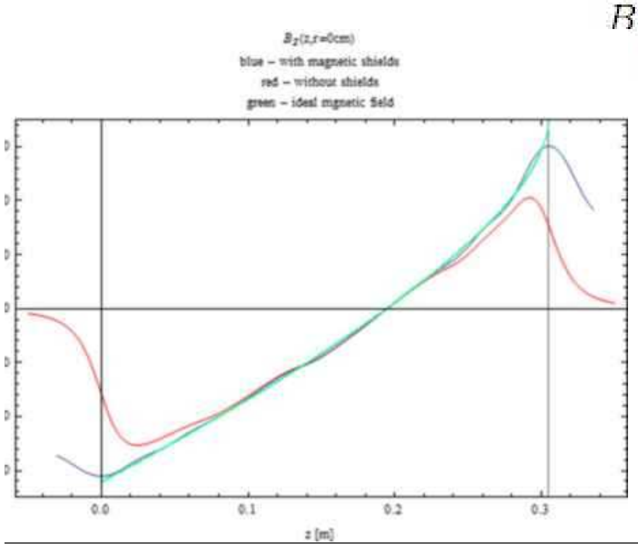

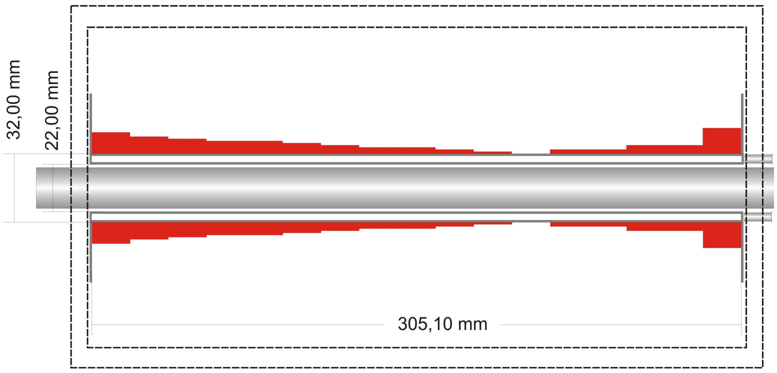

Transfer of atoms

Transfer of atoms from MOT to magnetic trap:

- atoms should not be lost nor heated – trap potentials should be well fitted.

MOT: gaussian shape of the atom cloud

$$n_{MOT}(\mathbf{r}) = n_0 \exp\left(-\frac{x^2+y^2}{\sigma_\rho^2} - \frac{z^2}{\sigma_z^2}\right)$$

Magnetic trap: what potential shape best preserves the phase-space density?

harmonic trap ? linear trap

Transfer of atoms

Best harmonic trap shape:

parameters such, that clud shape not altered

$$B'' = \frac{2k_B T}{g_F m_F \mu_B} \frac{1}{\sigma_z}$$

$$B''_\rho = \frac{B'^2}{B_0} - \frac{B''}{2} = \frac{2k_B T}{g_F m_F \mu_B} \frac{1}{\sigma_\rho^2}$$

$$\frac{B'^2}{B_0} = B''_\rho + \frac{1}{2} B'' = \frac{2k_B T}{g_F m_F \mu_B} \left(\frac{1}{\sigma_\rho^2} + \frac{1}{2\sigma_z^2} \right)$$

Caution: gravity!

Next step: adiabatic compression to increase density & collision rate.

Transport of atoms

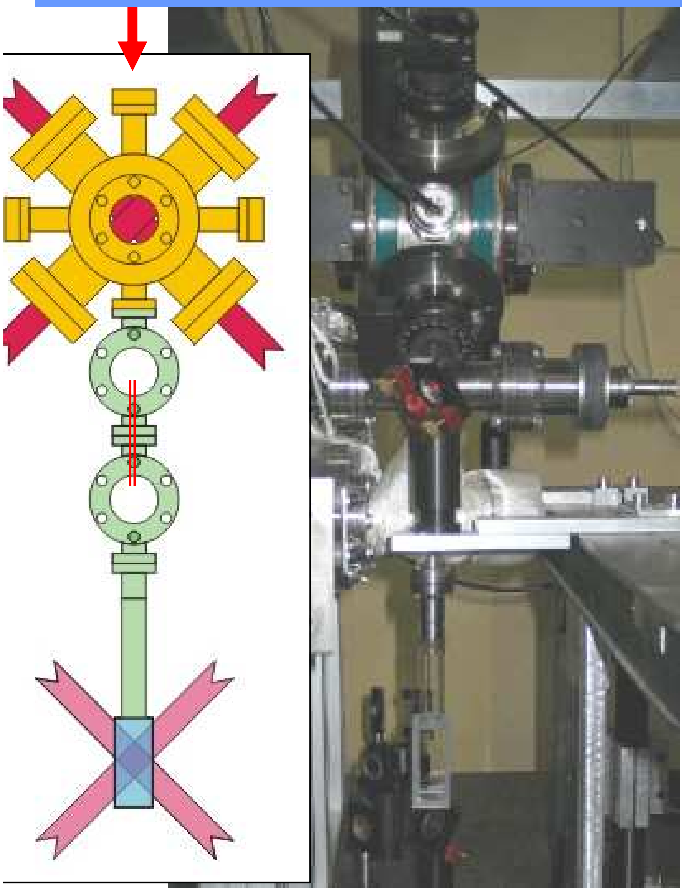

- why?

upper MOT:
a lot of atoms – pressure 10^{-7} mbar
lower MOT:
pressure < 10^{-10} mbar

- how?

light pressure
– pushing beam

- difficulties?

geometry of differential pumping
(distance 0,5 m, tube 5 mm, length 8 cm

atoms released from the upper MOT,
recaptured in the lower MOT

Pushing beam

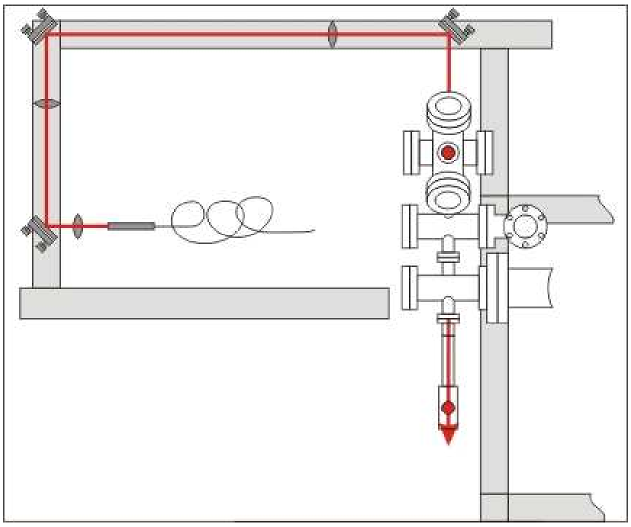

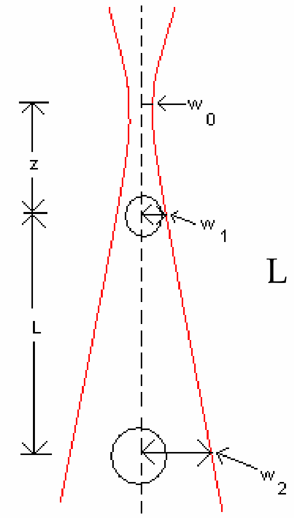

Upper MOT — high intensity, comparable to the trap beams: w_1=1,1mm.

Lower MOT — low intensity, no effect on the trap: w_2=3,3 mm

Atom collection

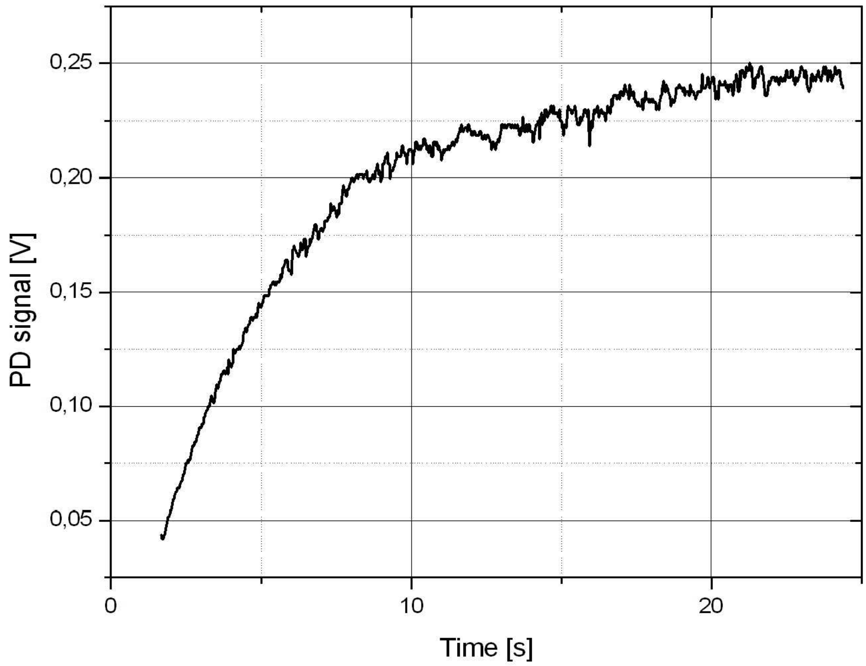

Loading of the lower MOT

Other possibilities

- cyclic transfer
- 2D MO traps

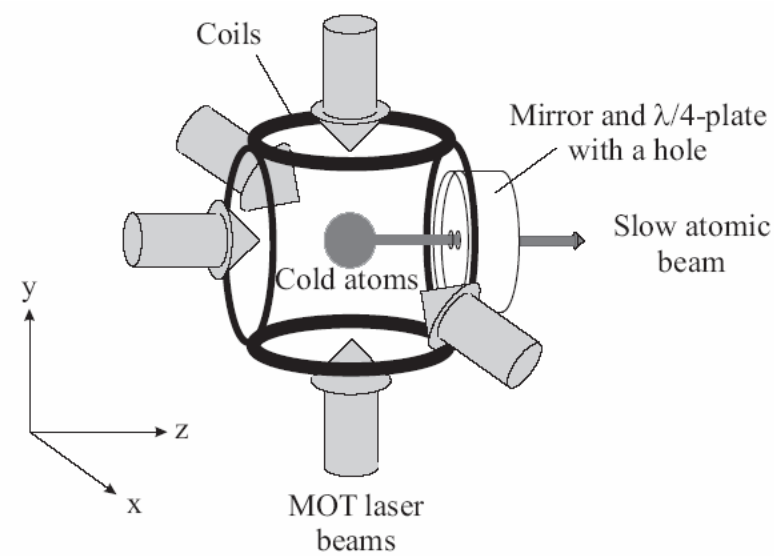

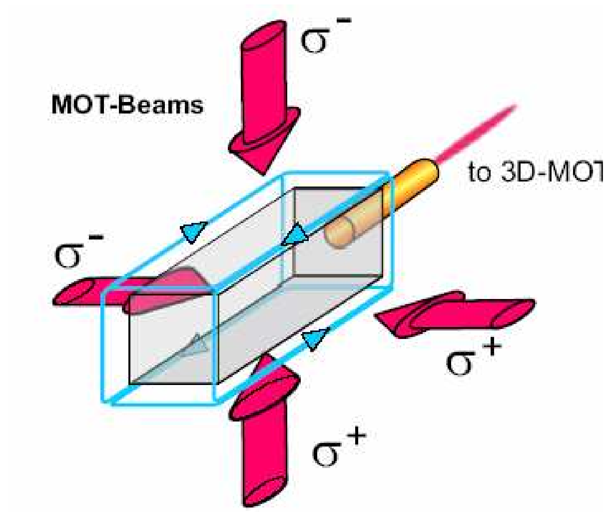

Other possibilities

- magnetic transport : system of quadrupole coils, sequential action

idea

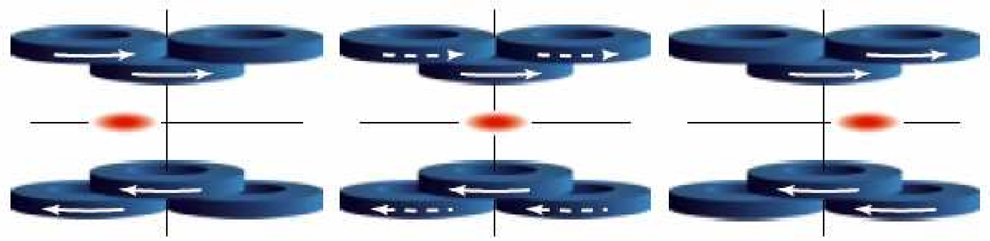

experimental setup

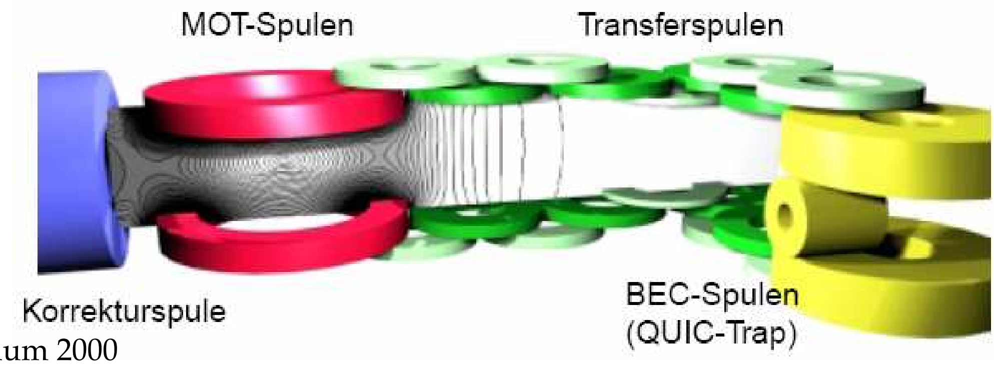

Greiner, Haensch, Monachium 2000

Other possibilities

- magnetic transport :
  moving magnetic trap on a linear track

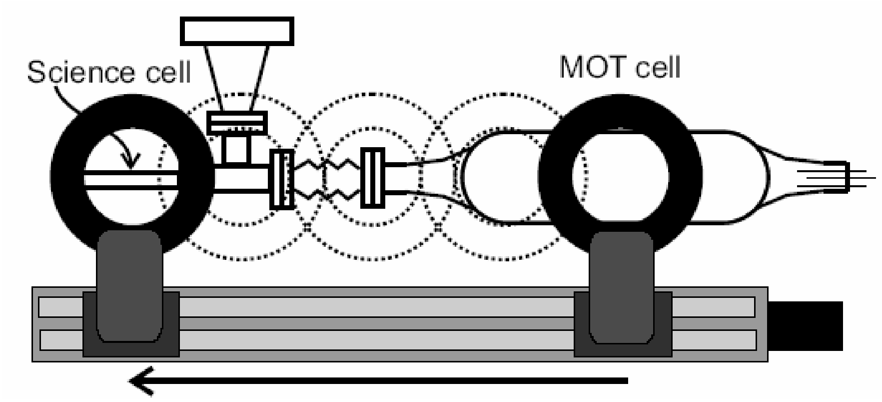

Lewandowski, Cornell, Boulder

Between MOT and MT

- Additional cooling and compression of atoms :
  - Cold MOT: higher detuning, lower intensity of laser beams,
  - Higher gradient of magnetic field,
  - Subdoppler cooling.
- Only certain magnetic states are trapped – optical pumping necessary.

Current control

Control of the currents in magnetic trap coils:

- currents tens to hundreds A,
- high power MOSFETs
- switching time: ms
- coil inductance!

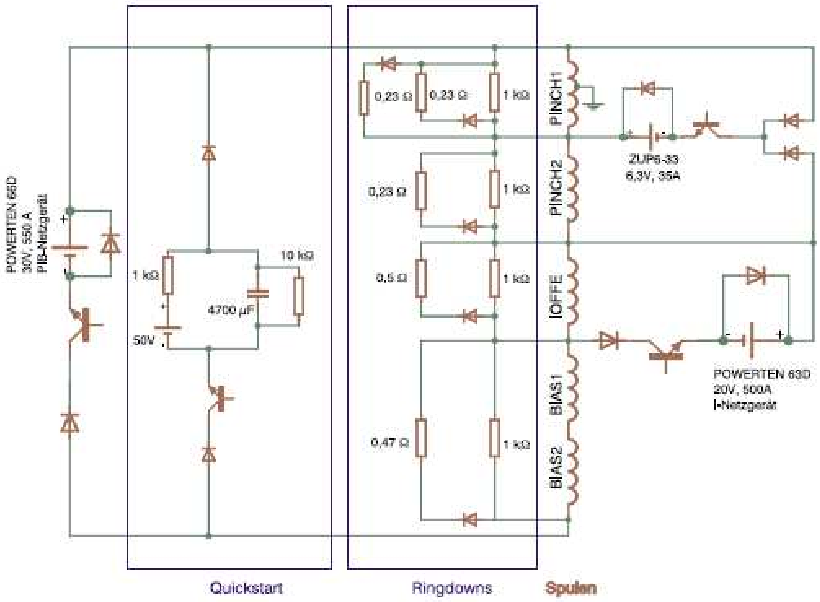

Experiment control

Elements under control:

- AOM frequencies
- switching on and off of AOMs
- shutters
- magnetic trap currents
- rf field frequency
- CCD camera trigger

Experiment control

- for convenience: two PCs
  - experiment control: timing, digital, analog, GPIB commands
  - camera control, aquisition and processing of images
- Real-time control Attention, operating system!
- Software.

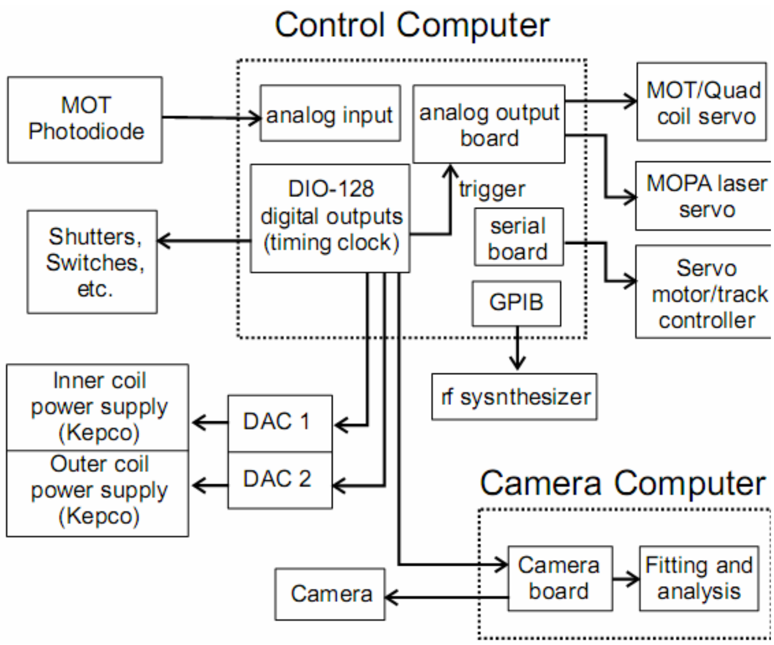

Detection

- A „probe" not possible
  probe of a size ~10µm: 10^{13} atoms — much more than sample size
- Optical methods:
  - photon absorption
  - photon reemission (fluorescence)
  - phase shift (dispersive imaging)

$$E(x,y) = tE_0(x,y)e^{i\Phi}$$

$$t = \exp\left(-\frac{\bar{n}\sigma_0}{2}\frac{1}{1+\delta^2}\right); \quad \Phi = -\frac{\bar{n}\sigma_0}{2}\frac{\delta}{1+\delta^2}$$

n column density, σ_0 cross-section, δ laser detuning

Optical detection

- Absorption methods — measure of t^2
- Dispersive methods:
  - phase modulation must be converted into intensity modulation,
  - separation of scattered light from direct light necessary,
  - dark field & phase contrast methods.

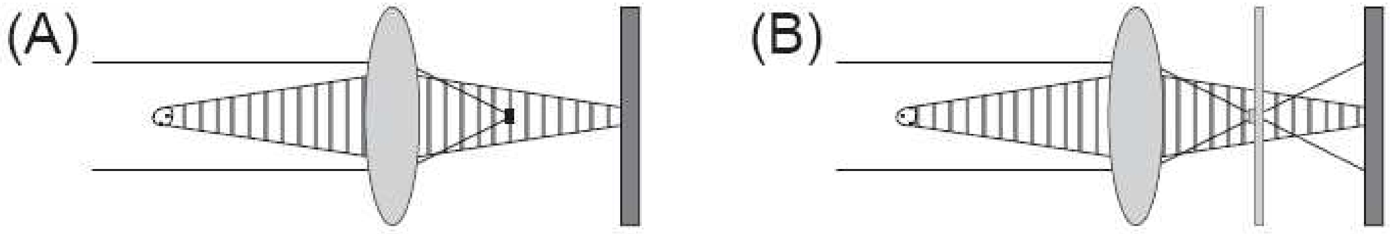

Absorption methods

- Small sample, high density, resonant light — total absorption,
- Atoms released from the trap and expanded:
  - smaller density and absorption,
  - measutement of initial velocity distribution.

Image analysis

Signal recorded by the camera :

$$F_I(x,y) = F_{I0}\left[P(x,y)e^{-D(x,y)} + S(x,y)\right] + N(x,y)$$

P beam profile, *S* scattered field, *N* background, *D* optical density

Two additional images recorded:

with laser beam, but without atoms:

$$F_B(x,y) = F_{I0}\left[P(x,y) + S(x,y)\right] + N(x,y)$$

without laser beam

$$F_D(x,y) = N(x,y)$$

Image analysis

Transmission $T(x,y)=t^2$:

$$T(x,y)=\frac{F_I(x,y)-F_D(x,y)}{F_B(x,y)-F_D(x,y)}$$

part of the image without atoms used to check if $F_{I0} \neq F_{B0}$

$$T(x,y)\approx e^{-D(x,y)}+\left[1-e^{-D(x,y)}\right]\frac{S(x,y)}{P(x,y)}$$

Beckground reduction difficult when vibrations occur